CHARLES UNIVERSITY

Faculty of science

Medicinal chemistry

Tomáš Svoboda

Toward Asymmetric Total Synthesis of Podophyllotoxin Derivatives

Přístup k asymetrické totální syntéze derivátu podophylotoxinu

Bachelor thesis

Supervisor: Dr. habil. Ullrich Jahn, Ph.D.

Consultant: Ing. Tomáš Mašek, Ph.D.

2023

Prohlášení

Prohlašuji, že jsem tuto závěrečnou práci vypracoval samostatně a že jsem uvedl veškeré použité informační zdroje a literaturu. Dále prohlašuji, že tato práci ani žádná podstatná část z ní nebyla použita k získání jiného nebo stejného akademického titulu. Jsme si vědom, že případné využití výsledků, získaných v této práci, mimo Univerzitu Karlovu, je možné pouze po písemném souhlasu této univerzity. Tato bakalářská práce byla vypracována na Ústavu organické chemie a biochemie AV ČR, v. v. i.

V Praze dne 21.5.2023 ………………………

Tomáš Svoboda

Acknowledgment

My deep gratitude belongs to my supervisor Tomáš Mašek, who without hesitation took the opportunity to be my mentor, and without expecting much in return, he taught me most of the things that I've learned during this long and difficult journey I've chosen to pursue. Not only did he help me with chemistry problems and correct my thesis, but also became one of my close friends and directed some of the actions in my personal life.

I would also like to thank to Dr. Ullrich Jahn, who has taken me under the wings of his research group and provided me with academic background. He also meticulously corrected my thesis, even under time pressure that we repeatedly experienced. He inspired me with his profound knowledge and the willingness to help with any problem.

Having worked here for a significant period of time, I would like to express my gratitude to the entire Institute of Organic Chemistry and Biochemistry, which was not only my workplace, it was also my school during COVID times, sanctuary during dark times and most importantly the place where I spent the best times of my life so far.

I would like to acknowledge the support from my closest friends, whose names I cannot include, as there is too much of them, who tirelessly supported me in my efforts to pursue all my actions, my first mentor Míra, who became my close friend and taught me many skills that I now possess of, including basic understanding of organic chemistry, my colleagues, who I spent time with during most of my worktime, and also my dearest girlfriend Tereza, who was strong enough to pursue this long journey by my side even in the dark times.

Finally, I need to express my deepest gratitude to my parents Tomáš and Martina, who effortlessly helped me achieve this success in any imaginable way. They wanted the best for me and without them I would not be able to finish this, therefore I thank them.

Abstract

Podophyllotoxin is a naturally occurring lignan with a wide range of biological activities, including anti-cancer and anti-viral properties. Total synthesis of podophyllotoxin has been a long-standing challenge in organic synthesis due to its complex and highly functionalized structure. In this work, we present our approach toward the total synthesis of podophyllotoxin using a fully stereoselective strategy.

Our approach involves the enantioselective vinylation of 2-bromo-piperonal followed by a stereoselective conjugate addition reaction combined with the addition of methylene unit and a metathesis reaction, that provides starting material for another conjugate addition, which could lead to the target. The key step of our synthesis is the stereoselective conjugate addition of an organolithium to an α,β-unsaturated ester, which leads to the formation of a chiral quaternary center with high selectivity and metathesis that successfully joins parts into the desired cycle.

Despite the success of our strategy in achieving the desired stereoselectivity, we encountered some challenges in the subsequent steps of the synthesis, which prevented us from completing the total synthesis of podophyllotoxin. However, our results demonstrate the potential of enantioselective vinylation and stereoselective conjugate addition reactions in the total synthesis of complex natural products.

Future studies will focus on optimizing the reaction conditions and developing new strategies to overcome the remaining challenges in the total synthesis of podophyllotoxin. Overall, our work provides valuable insights into the development of new methods for reaching not only podophyllotoxin, but also the synthesis of complex natural products and will inspire new directions for future research in this field.

Abstrakt

Podophylotoxin je přirozeně se vyskytující lignan se širokou škálou biologických aktivit, včetně protirakovinných a antivirových vlastností. Celková syntéza podophylotoxinu je dlouhodobou výzvou v organické syntéze díky své komplexní a vysoce funkcionalizované struktuře. V této práci prezentujeme náš přístup k celkové syntéze podophylotoxinu pomocí zcela stereoselektivní strategie.

Náš přístup zahrnuje enantioselektivní vinylaci trimethoxyvinylsilanu následovanou stereoselektivní konjugovanou adicí kombinovanou s přidáním methylenové jednotky a metatézní reakcí, která poskytuje výchozí materiál pro další konjugovanou adici, která zakončí celou syntézu. Klíčovým krokem naší syntézy je stereoselektivní konjugovaná adice organolithiu k α,β-nenasycenému esteru, což vede k vytvoření chirálního kvartérního centra s vysokou selektivitou a metatezí, které úspěšně spojuje části do požadovaného cyklu.

Navzdory úspěchu naší strategie při dosahování požadované stereoselektivity jsme se v následných krocích syntézy setkali s některými problémy, které vedly k podophylotoxinu. Naše výsledky však prokazují potenciál enantioselektivní vinylace a stereoselektivních konjugovaných adičních reakcí v celkové syntéze komplexních přírodních produktů.

Budoucí studie se zaměří na optimalizaci reakčních podmínek a vývoj nových strategií k překonání zbývajících problémů v celkové syntéze podophylotoxinu. Celkově naše práce poskytuje cenné poznatky o vývoji nových metod pro dosažení nejen podophylotoxinu, ale syntézy komplexních přírodních látek a bude inspirovat nové směry pro budoucí výzkum v této oblasti.

1 INTRODUCTION **11**

1.1 STRUCTURE OF PODOPHYLLOTOXIN[1, 2, 3] **11**
1.2 PODOPHYLLOTOXIN ORIGIN AND HISTORY **11**
1.3 PODOPHYLLOTOXIN EFFECTS AND CHINESE MEDICINE **12**
1.4 PODOPHYLLOTOXIN IN PLANTS **13**
1.5 GENERAL BIOACTIVITY[1] **14**
1.5.1 BREAST CANCER 14
1.5.2 LUNG CANCER [9] 15
1.5.3 COLORECTAL CANCER [9] 16
1.6 LIGNAN CLASSIFICATION **16**
1.6.1 ARYLNAPHTALENE STRUCTURE GROUP 17
1.6.2 ARYLTETRALIN STRUCTURE GROUP 17
1.6.3 DIBENZOCYCLOOCTADIENE STRUCTURE GROUP[13] 17
1.6.4 DIBENZYLBUTANE STRUCTURE GROUP [15] 18
1.6.5 DIBENZYLBUTYRLACTONE STRUCTURE GROUP [16,17] 18
1.6.6 FURANOID STRUCTURE GROUP [18] 19
1.7 BIOSYNTHESIS[1] **19**
1.8 STRUCTURE-ACTIVITY RELATIONSHIPS **21**
1.8.1 RING A MODIFICATIONS [21] 21
1.8.2 RING C MODIFICATIONS 22
1.8.3 C7-O MODIFICATIONS[25] 22
1.8.4 C7-N MODIFICATIONS 23
1.8.5 RING D MODIFICATIONS **24**
1.9 APPROVED DRUGS **24**
1.9.1 ETOPOSIDE [28] 24
1.9.2 TENIPOSIDE [18] 25
1.9.3 PODOFILOX 25
1.10 KNOWN SYNTHETIC APPROACHES TO PODOPHYLLOTOXIN. 25
1.11 SYNTHETIC METHODOLOGY **26**
1.11.1 OLEFIN METATHESIS 26
1.11.2 CONJUGATE ADDITION 27

2 AIMS OF THE WORK 29

3 EXPERIMENTAL PART 30

3.1 (S)-1-(6-BROMOBENZO[D][1,3]DIOXOL-5-YL)PROP-2-EN-1-OL (2) 30
3.2 TRANS-3,4,5-TRIMETHOXYBENZYL-TBU-PROP-2-ENOATE (3) 31
3.3 (S)-1-(6-BROMOBENZO[D][1,3]DIOXOL-5-YL)PROP-2-EN-1-OL (2E) 32
3.4 TERT-BUTYL (R*)-3-(6-{(S)-1-[(METHYLOXY)METHOXY]ALLYL}BENZO[D][1,3]DIOXOL-5-YL)-3-(3,4,5-TRIMETHOXYPHENYL)PROPANOATE (4) 33
3.5 TERT-BUTYL (3R*)-2-((DIMETHYLAMINO)METHYL)-3-(6-((S*)-1-(METHOXYMETHOXY)ALLYL)BENZO[D][1,3]DIOXOL5-YL)-3-(3,4,5-TRIMETHOXYPHENYL)PROPANOATE (5) 34
3.6 TERT-BUTYL (3R*)-3-(6-((S*)-1-(METHOXYMETHOXY)ALLYL)BENZO[D][1,3]DIOXOL-5-YL)-2-(METHOXYMETHYL)-3-(3,4,5-TRIMETHOXYPHENYL)PROPANOATE (6) 35
3.7 TERT-BUTYL-2-((R*)-(6-((S*)-1-(METHOXYMETHOXY)ALLYL)BENZO[D][1,3]DIOXOL-5-YL)(3,4,5-TRIMETHOXYPHENYL)METHYL)ACRYLATE (7) 37
3.8 TERT-BUTYL (5R*,8S*)-8-(METHOXYMETHOXY)-5-(3,4,5-TRIMETHOXYPHENYL)-5,8-DIHYDRONAPHTHO[2,3-D][1,3]DIOXOLE-6-CARBOXYLATE (8) 38

4 RESULTS AND DISCUSSION 40

5 CONCLUSION 52

6 REFERENCES 53

List of abbreviations and symbols

RCM.. Ring-closing metathesis

CM .... Cross-metathesis

THF .... Tetrahydrofuran

BuLi .... butyllithium

approx. .... Approximately

DIPEA... N,N-Diisopropylethylamin

TBAI .... tetra-n-butylammonium iodide

Equiv. .... Equivalents

TLC .... Thin layer chromatography

R_f .... Retention factor

IR (w, m, s, vs, b) .... Infrared (weak, medium, strong, very strong, broad)

NMR .... Nuclear magnetic ressonance

MS... Mass spectroscopy

Ar .... Aryl

^{p}O, ^{m}O .... para-O, meta-O

EtOAc .... Ethyl acetate

PE .... Petroleum ether

MOM .... Methoxymethyl

dr .... diastereomer ratio

TMP .... tetramethylpiperidine

HDMS... bis(trimethylsilyl)amide

TMEDA .... tetramethylethylendiamine

BINAP .... (2,2′-bis(diphenylphosphino)-1,1′-binaphthyl)

SEGPHOS .... 3,5-dimethylphenyl and 3,5-di-tert-butyl-4-methoxyphenyl

MDMA .... methylendioxymethamphetamine

Me .... Methyl

Et .... Ethyl

HG .... Hoveyda-Grubbs

PG .... Protecting Group

Ar .... Aryl

NHC .... N-heterocyclic

COMMON LATIN ABBREVIATIONS

e.g.	"exempli gratia." for example
in vitro	performed in a test tube, culture dish, or elsewhere outside a living organism
in vivo	performed in a living organism.
in situ	situated in the original place.
in vacuo	in a vacuum
et al.	"et alii" and others

1 Introduction

1.1 *Structure of podophyllotoxin*[1, 2, 3]

(-)-Podophyllotoxin **1** is a natural product and secondary metabolite of various plants. The scaffold of **1** contains two phenylpropanoid units (cinnamic acid/alcohol residues) connected via 8-8' linkage (see fig. 1). The two units differ in their oxidation state and substitution pattern on the phenyl rings. Cyclolignans in contrast to lignans contain also 2-7' bond, that forms ring C (see fig. 1). As a characteristic of cyclolignans, **1** possesses typical lignan features, including a carbocycle formed by two single bonds that connect both phenylpropanoid units between 8 and 8', as well as a bond between 2 and 7' carbon. Positioned at the 8 and 8' of ring C, **1** exhibits additional distinctive features such as a 1,2,3,4-tetrahydronaphtalene core, a 3,4,5-trimethoxyphenyl group at position 7', and a butyrolactone ring fused to the aforementioned positions. The *trans* fusion of rings C and D is crucial for biological activity. The whole structure contains 4 chiral centers which in particular influence the mechanism of action. The hydroxy function at position 7 and its substitution play an important role in protein-ligand interaction.

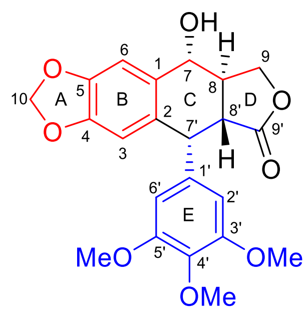

1
Podophyllotoxin

Figure 1: Podophyllotoxin structure and typical lignan-like numbering.

1.2 *Podophyllotoxin origin and history*

Origins of **1** can be traced back to ancient times, where it was first discovered in certain plant species. It can be found e.g., in *Dysosma versipellis, Diphylleia sinensis, Sinopodophyllum hexandrum* and other plants all over the world but the most common sources are the rhizomes of *Podophyllum Peltatum* (*American mayapple*) and the *Sinopodophyllum hexandrum (Himalayan mayapple)* found in the region of western China and the Himalayas [1, 2]. The pure compound is predominantly obtained from an alcoholic extract of podophyllum species called podophyllin. Podophyllum species were first described by Swedish botanist C. Linaeus[4] but the compound itself was first isolated in 1880 by V. Podwyssotzki at the University of Dorpat (nowadays Tartu, Estonia). The structure wasn't known until 1930 when W. Borsche and J. Niemann suggested an ultimately incorrect structure [5]. The correct structure was elucidated 20 years later by A. Schrecker and J. Hartwell by means of chemical degradation [6]. However, the medicinal properties of **1** in the form of podophyllin resin have been known for a long time. Preparations of **1** were described in Chinese medicine books hundreds of years old. Western medicine discovered podophyllin in the 19th century when it was included in the first U.S. Pharmacopoeia in 1820 and was retained until the twelfth revision in 1942. It has at some point appeared in most European, South American, and Asian Pharmacopoeias[7]. The pure form of **1** was discovered roughly in the 1940s when it was introduced as a treatment for *Condyloma accuminata* (HPV – human papillomavirus) and *Verruca vulgaris* (warts manifestation caused by HPV) [8].

1.3 Podophyllotoxin effects and Chinese medicine

People from many places and ethnicities throughout history independently found out that these plants had healing effects and used them for this purpose. Ancient healers used the plants and predominantly their alcoholic extract podophyllin for a broad range of human health problems. It was later found that **1** exhibits antitumor, antibacterial, antiviral, immunosuppressive, analgesic, antioxidative as well as anti-inflammatory and antiasthmatic[2] effects, lending modern scientific explanation for its widespread use against a range of illnesses and diseases. Plants containing **1** such as *Bajiaolian* or *Chinese mayapple* are in Chinese books described as a remedy for snake bites, weakness, *Condyloma accuminata*, tumors, lymphadenopathy, and other disorders[9], however, resin application can be accompanied by negative side effects. After drinking *Bajiaolian* blends the reported manifestations are not only nausea, vomiting, diarrhoea and abdominal pain, but also thrombocytopenia, leucopenia, peripheral tingling or numbness, sensory ataxia, abnormal liver function, and disturbance of consciousness. Interestingly, the literature reports poisonings from topical use or accidental ingestion of Podophyllin resin, but no case of lethal poisoning from drinking infusions of crude plant blends has been reported. It's known that cow milk from cows grazing on the land inhabited by these plants tends to be extremely cathartic. The main active ingredient of Podophyllin resin is known to be **1** accompanied by deoxypodophyllotoxin, β-sitosterol, astragalin (see fig. 2), reaching up to other 16 substances. The rhizome of plants contains roughly 2-4% of resin by dry weight which itself contains approximately 20% of **1**. The plant is traditionally sliced or smashed and extracted by water or ethyl alcohol. Conventional methods stated in books recommend loading 5 to 50 g of the rhizomes, which corresponds to approximately 20 to over 200 mg of **1**, depending on the content in the plant. Loading values are stated in books as in therapeutic range but the amount can actually cause severe toxicity. The acute symptoms developed during acute poisoning include nausea, vomiting, diarrhoea, and leukocytosis followed by leucopenia, prolonged areflexia, sensory ataxia, fever, memory impairment, visual and auditory hallucinations, paranoia, fainting, and coma. These clinical manifestations of Podophyllin correlate with **1** intoxication, from which can be concluded that the active ingredient of Podophyllin is **1**. The treatment of acute poisoning is principally supportive. There is no conclusive information regarding the usefulness of hemoperfusion as it was only useful in 60% of cases during which hemoperfusion was applied.

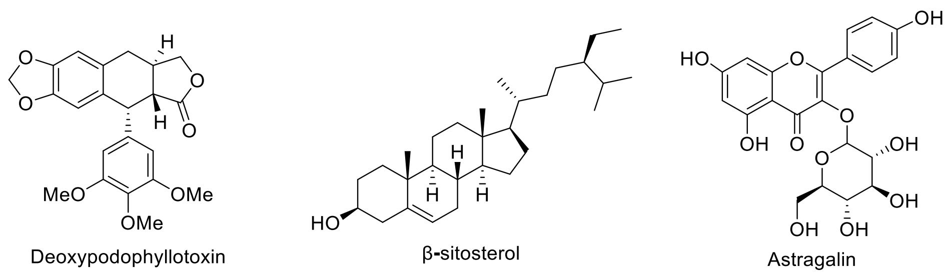

Figure 2: Structure of compounds found in Podophyllin resin.

1.4 Podophyllotoxin in plants

The highest amounts of **1** contain three genera from the *Berberidaceae* family. Those genera are namely *Dysosma woodson*, *Diphylleia michx, and Sinopodophyllum ying* and contain mostly between 2.7–4.2% of the dry weight but reaching up to 9.58% which was measured in *Sinopodophyllum hexadrum* collected in western China. Traces of **1** can be find also in *Thuja*, *Callitris, Thujopsis, Hernandia, Juniperus, Nepeta,* and *Thymus*, but concentrations are considerably lower than in the *Berberidaceae* family. The highest concentration of resin is in the roots and rhizomes of plants but the whole plant is poisonous. Most of the plants that contain **1** in high concentrations need 5-7 years of growth to be harvested. Those plants also have very low reproducing ability, therefore these plants are close to extinction for the reason of overexploitation.

American mayapple is a spring wildflower that produces a single, nodding white flower under umbrella-like leaves in April (see fig. 10). These plants only bloom when mature enough to produce two leaves per stem. The flower develops into an edible, greenish fruit, turning golden when ripe, and is used for preserves. All other parts of this plant are poisonous. By the end of June, this species has gone dormant. Native to much of the eastern US, it prefers rich, moist soil but is also tolerant of poor soil conditions and drought. It mostly grows in areas that are devoted almost exclusively to mayapple, as it tends to colonize shady areas.

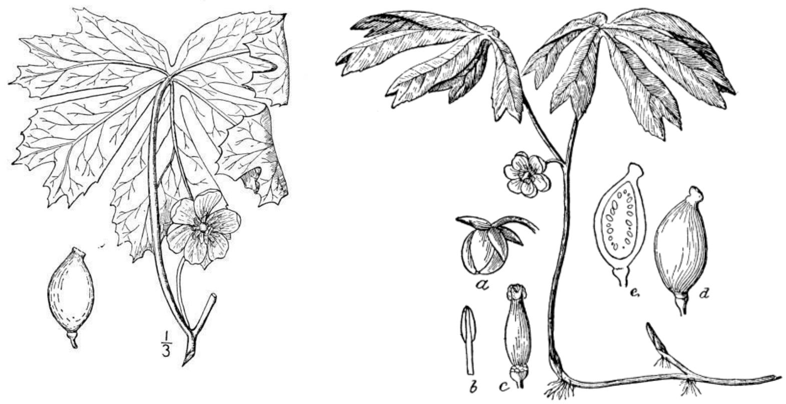

Figure 10: American Mayapple schematic drawing.

Plants containing **1** do share morphological signs thus do belong to obvious morphological kindship of *Podophyllum*, *Diphylleia*, and *Hydrastis*. Therefore, they are corroborated by alkaloid chemistry. Plant itself is highly toxic, which is caused by the presence of Podophyllin resin. Rhizomes, leaves, and stems contain high concentrations as well as unripe fruit, but once the fruit is fully ripe, it is not toxic anymore.

Sinopodophyllum genus is a rhizomatous perennial with creeping rootstocks producing 2-branched petioles, each branch bearing a large, usually peltately divided, umbrella-like leaf blade. 9-petalled, cup-shaped flowers are borne on short stems from the junction of the leaf branches, followed by red or yellow fruit

1.5 General bioactivity[1]

The main effects that **1** exhibit in a cell is the ability to arrest the cell cycle in the S phase, target the colchicine binding domain with the 3,4,5-trimethoxyphenyl unit of the E ring, and the effect of inhibition of topoisomerase II enzyme that cuts both strands of DNA helix simultaneously to manage DNA tangles and supercoils. **1** is highly *in vivo* toxic, therefore it cannot be administered orally nor by injection. **1** was recently used for the treatment of cytokine storm during COVID-19 infection. All naturally occurring **1** derivatives have low bioavailability and considerable systemic toxicity such as neurotoxicity, hair loss, gastrointestinal toxicity, and bone marrow suppression. These natural compounds also very quickly induce drug resistance, therefore **1** was used as a starting point for finding novel, less toxic derivatives rather than being used for therapeutic purposes.

1.5.1 Breast cancer

According to ECIS (European Cancer Information Systém), „One of the most prevalent cancers worldwide is breast cancer. Over 12% of all women in the United Stated experience invasive breast cancer in their life. Almost 3.8 million women had this type of cancer by the time of January 2022. The U.S. World Health

Organization postulated that the incidence of breast cancer in Europe in 2022 was almost 600 000. Breast cancer is also the leading cause of women's death linked to cancer worldwide, accounting for 16%".

Many **1** derivatives can effectively inhibit the proliferation, migration, and invasion of cancer cells *in vitro* and *in vivo* making it a promising treatment for this type of cancer. Compounds were observed to cause damage to the human breast cancer cell line (MCF-7) by blockade of the G2/M cell cycle and distortion of microtubules. No damage was detected against the non-cancerous cells. Different derivatives stopped the growth of cancerous cells by the increase of p53 expression, cyclin B1 protein expression, and decrease in Cdk1, so the mechanism of action is probably somehow connected to mitosis. Proteins regulating the tumor microenvironment were observed to be affected, therefore **1** derivative can influence the angiogenesis of tumors. At least one **1** derivative also had significant cytotoxic activity against cancer cells utilizing different mechanisms. It led to the formation of ROS particles, ATM/p53/p21 pathway distortion followed by DNA damage in cancerous cells, and mitochondrial apoptosis along with the cell cycle arrest.

1.5.2 Lung cancer [9]

According to ECIS (European Cancer Information Systém), „In 2020 was estimated lung cancer accounted for 11.9% of all new cancer diagnoses (excluding non-melanoma skin cancers) and 20.4% of all deaths due to cancer in european countries. That made it the fourth most frequently occurring cancer (after prostate, breast, and colorectal cancers) and the leading cause of cancer death."

Various studies concluded that **1** derivatives have the potential for inhibition of the growth of lung cancer utilizing ROS production and G2/M cell cycle blockade. It was found that c-MET (tyrosine-protein kinase MET) inhibition caused apoptosis that can be explained by **1** presence [19]. Semi-synthetic compound Apopicropodophyllotoxin (see fig. 11) has also high cytotoxic activity against lung cancer cells. It leads to the accumulation of CHK21 and phosphorylated p21 and Cdc2 proteins that discombobulate microtubule polymerization and therefore cause DNA damage. It also led to the activation of the caspase (-3, -8, -9) pathway.

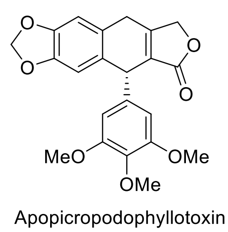

Figure 11: Structure of Apopicropodophyllotoxin.

1.5.3 Colorectal cancer [9]

According to ECIS (European Cancer Information Systém), “It is estimated that in 2020, colorectal cancer accounted for 12.7% of all new cancer diagnoses and 12.4% of all deaths due to cancer in European countries. That made it the second most frequently occurring cancer (after breast cancer) and the second cause of cancer death (after lung cancer)”

CRC cell lines are usually used for pharmacology studies. **1** derivatives were found to be effective for all 7 major types of CRC cell lines. A mechanism is targeting Topoisomerase II and G2/M cell cycle arrest resulting in cell apoptosis. Western blotting showed that cell cycle arrest was associated with a decrease in cdc2 kinase activity and increased cdc2 phosphorylation. A regular chemotherapeutic agent used for the treatment of colorectal cancer is 5-Flurouracil (5-FU), it however causes considerable resistance. It was shown that deoxypodophyllotoxin (see fig. 2) showed relevant inhibitory activity against the 5-FU resistant cell lines in *in situ* mouse model, where it effectively stopped metastasis[20].

1.6 Lignan classification

Lignans are composed of phenylpropanoid units, specifically cinnamic acid. Biosynthetically they come from tyrosine and phenylalanine amino acids. Those units also form lignin – a pre-eminent polymer in the plant cell walls forming wood. Wood in Latin is “ligna”, hence the name. Lignan name is usually restricted to a 2-unit dimer connected via 8-8’ linkage. Molecules formed by alternative coupling are called neolignans. Lignans can also be subdivided into Cyclolignans, a cyclized lignans containing 2-7’ bond or Oxyneolignans with the presence of oxygen (see fig. 3). Lignans can be classified into eight subgroups: arylnaphthalenes, aryltetralins, dibenzocyclooctadienes, dibenzylbutanes, dibenzylbutyrolactones, dibenzylbutyrolactols, furans, and furofurans. The phenylpropanoid dimer can be post-processed in the plant to varying degrees of oxidation.

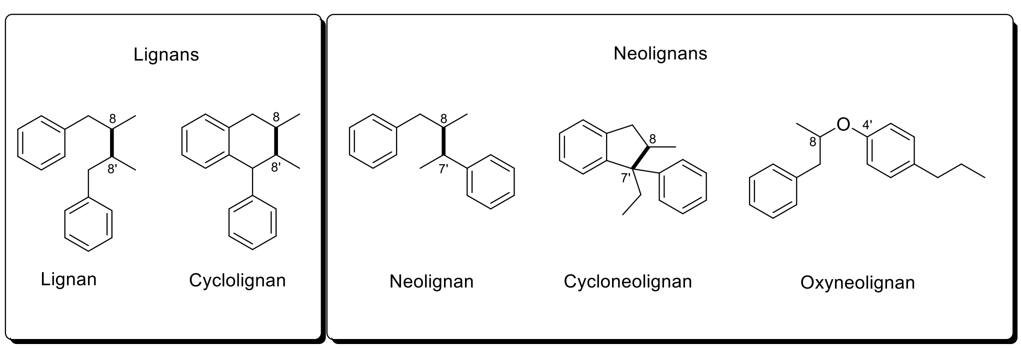

Figure 3: Lignan structural division. The bold bond illustrates the position of lignan coupling.

1.6.1 Arylnaphtalene structure group

The most important compounds from Arylnaphtalene group are Diphyllin and Justicidin B (see fig. 4) with antiviral and antiproliferative effects [10,11]. Diphyllin is also known as an effective inhibitor of Severe Acute Respiratory Syndrome Coronavirus 2 (SARS-CoV-2). Arylnaphthalene lignans are characterized by unsaturated 7−8 and 7′−8′ bonds. Arylnaphtalenes are widely distributed in Linum (flax) species. Exhibiting noteworthy analgesic and anti-inflammatory properties, Sevanol, a naturally occurring lignan extracted from Thymus armeniacus, effectively hinders the activity of ASIC1a and ASIC3 amiloride-sensitive cation channel isoforms[12].

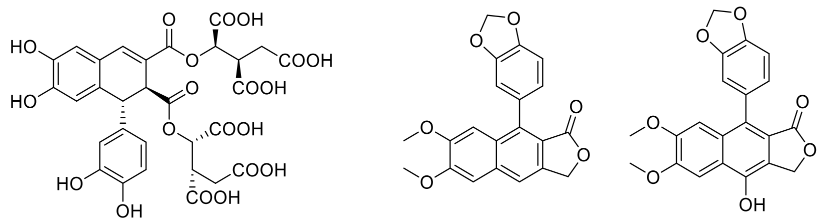

Sevanol
Arylnaphtalene structure group

Justicidin B

Diphyllin

Figure 4: Sevanol, Justicidin B and Diphyllin structures.

1.6.2 Aryltetralin structure group

Even though lignans are found in over 70 families of plants, aryltetralins were only found in a few. The two most important aryltetralins are **1** and β-peltatine (see fig. 5). Both of those have anticancer and antimitotic properties.

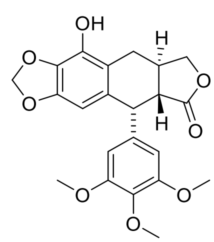

β-peltatine
Aryltetraline group

Figure 5: Aryltetraline group.

1.6.3 Dibenzocyclooctadiene structure group[13]

Dibenzocyclooctadienes are found in the genus *Kadsura* (*Schisandraceae* family) of plants distributed in Asian countries. The group is not well explored, though a couple of compounds such as Gomisin A (see fig. 6) are known and were isolated and well characterized. Compounds also exerted various beneficial biological activities such as anti-inflammatory and cytotoxic activities, as well as being potent antiviral agents. Gomisin A, in animal models of acute hepatic injury, has demonstrated the ability to enhance hepatocyte growth factor, restrain lipid peroxidation, and impede apoptosis. Additionally, it exhibits anti-inflammatory properties by inhibiting the release of arachidonic acid from macrophages [14].

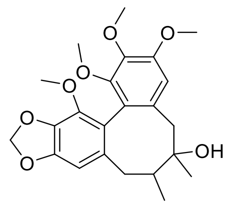

Figure 6: Structure of Dibenzocyclooctadiene lignan Gomisin A.

1.6.4 Dibenzylbutane structure group [15]

Dibenzylbutane lignans are two benzyl units connected via a butane linker. *E.g.* Nordihydroguaiaretic Acid (see fig. 7) and its derivatives belong to the group and can be found in leaves and twigs of the evergreen desert shrub *Larrea tridentata*. The compound has antioxidant and anti-inflammatory properties and can therefore easily quench hydroxy radicals generated via the Fenton reaction. It also showed cytotoxic properties in mice, where it activated the MAP kinase pathway causing apoptosis of pro-B lymphocytes and evoke cell death inducing oxidative damage of proteins in the medulloblastoma-derived Daoy cell line.

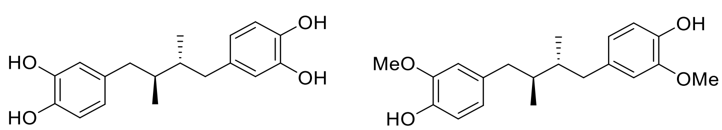

Figure 7: Meso-dihydroguaiaretic acid and Nordihydroguaiaretic acid structures.

1.6.5 Dibenzylbutyrlactone structure group [16,17]

Dibenzylbutyrlactone lignans come from plants and exert antioxidant, anti-inflammatory, antimicrobial, and antitumor properties. Arctigenin (see fig. 8) was isolated from *Torreya nucifera* barks but can be found in a variety of plants including *Bardanae fructus* (Goboshi), *Saussurea medusa* (Compositae), and more. Arctigenin was found to inhibit the replication of the human immunodeficiency virus, whereas savinin, a butyrolactone lignan from *Pterocarpus santalinus* was found to inhibit tumor necrosis factor-a (TNF-a) production and T-cell proliferation. Lactone-containing molecules exhibit a greater antitumor potency. However, lactones can be easily metabolized in the gastrointestinal tract by esterases, which decompose the molecule. Most of the structures of this group vary mostly just in ring A and ring B.

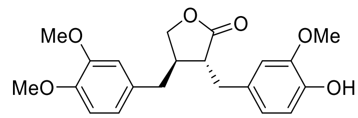

Figure 8: Dibenzylbutyrlactone lignan Arctigenin structure.

1.6.6 Furanoid structure group [18]

(+)-9'-isovaleroxylariciresinol (see fig 9) was obtained from *Valeriana jatamansi* plant. The compound was found to have significant in vitro cytotoxic activity against metastatic prostate cancer cell lines and colon cancer cell lines with IC_{50} of 8.1 and 5.3 mM respectively. Tripterygiol lignan, which was isolated from the *Tripterygium wilfordii* exhibited various activities including downregulation of cyclooxygenase-2 (COX-2), inducible nitric oxide synthase (iNOS) and interleukin-1b (IL-1b) gene expressions in a dose-dependent manner in LPS-elicited mouse macrophages.

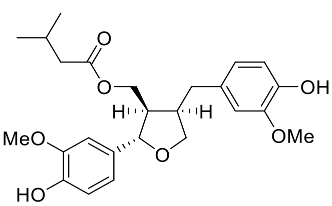

Figure 9: Furanoid lignan (+)-9'-isovaleroxylariciresinol structure.

1.7 Biosynthesis[1]

The first step of biosynthesis is the deamination of phenylalanine **I** which is the starting substrate for the whole biosynthesis via phenylalanine ammonia-lyase **PAL** enzyme forming cinnamic acid **II**. The latter is then converted with a series of enzymes via *p*-coumaric acid, caffeic acid caffeoyl CoA, and feruloyl CoA into the coniferyl aldehyde **III,** which is then reduced forming coniferyl alcohol **IV** via cinnamyl alcohol dehydrogenase **CAD** enzyme.

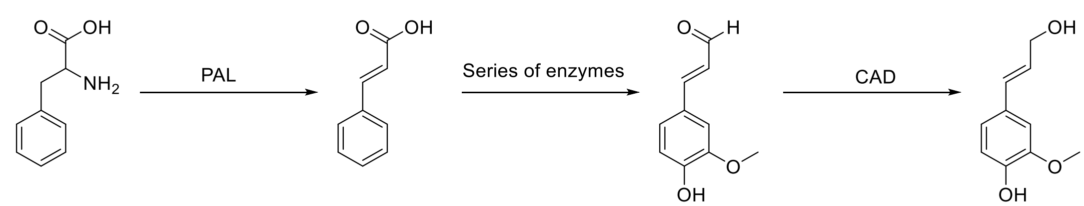

I II III IV

Scheme 1: Biosynthetic pathway from phenylalanine I to coniferyl alcohol IV.

Stereoselective coupling of two coniferyl alcohol **IV** molecules yields one molecule of (+)-pinoresinol **V** which is the step with the highest structure complexity increase. It sets two new stereocenters to the molecule. Stereoselectivity is mediated by the dirigent protein **DIR** which is not an enzyme as it does not have any actual enzymatic activity, however, it attaches substrates in a certain stereoselective manner. (+)-pinoresinol **V** is then reduced by a ring-opening mechanism with pinoresinol-lariciresinol reductase **PLR**, forming (+)-lariciresinol **VI.** The molecule has one free hydroxyl group and is then transformed into the secoisolariciresinol **VII,** which is a molecule with both rings opened into 2 free hydroxyl groups utilizing the same enzyme **PLR**.

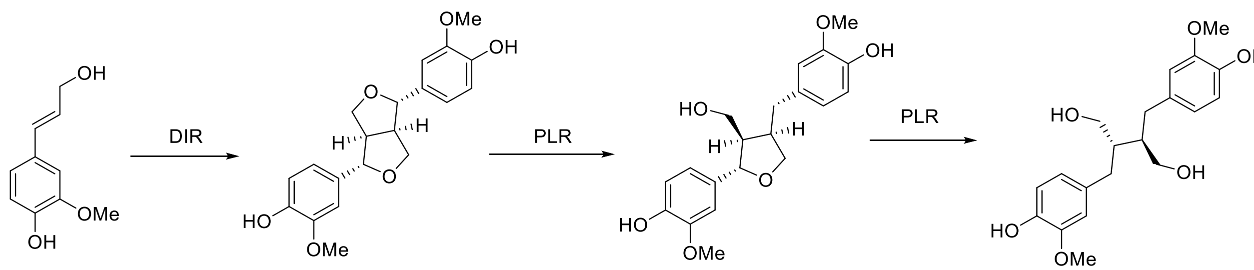

IV V VI VII

Scheme 2: Biosynthetic pathway from coniferyl IV alcohol to secoisolariciresinol VII.

Secoisolariciresinol dehydrogenase **SDH** then transforms **VII** to the matairesinol **VIII** with lactone ring D being formed. The latter is then transformed into pluviatolide **IX** which already has podophyllotoxin-like ring A formed. Pluviatolide is then methylated on the hydroxyl group located on the ring E with O-methyltransferase 3 **OMT3** yielding 5’-desmethoxy-yatein **X**.

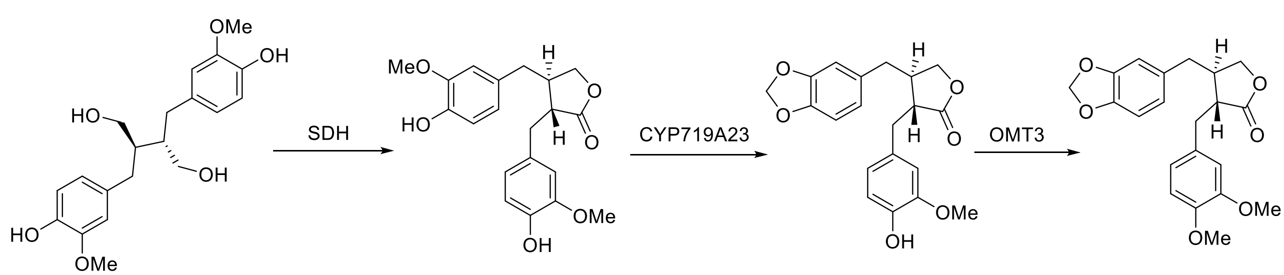

VII VIII IX X

Scheme 3: Biosynthetic pathway from Secoisolariciresinol VII to 5'-desmethoxy-yatein X.

5’-desmethoxy-yatein **X** is methoxylated in the ring E forming a typical podophyllotoxin-like 3,4,5-trimethoxybenzyl unit with o-methoxytransferase 1 **OMT1** forming Yatein **XI.** 2-oxoglutarate/Fe(II)-dependent dioxygenase **2-ODD** then cyclizes ring C which forms the deoxypodophyllotoxin scaffold. **XII** is hydroxylated on position 7 with yet unknown enzymatic reaction sequence forming the final product of biosynthesis.

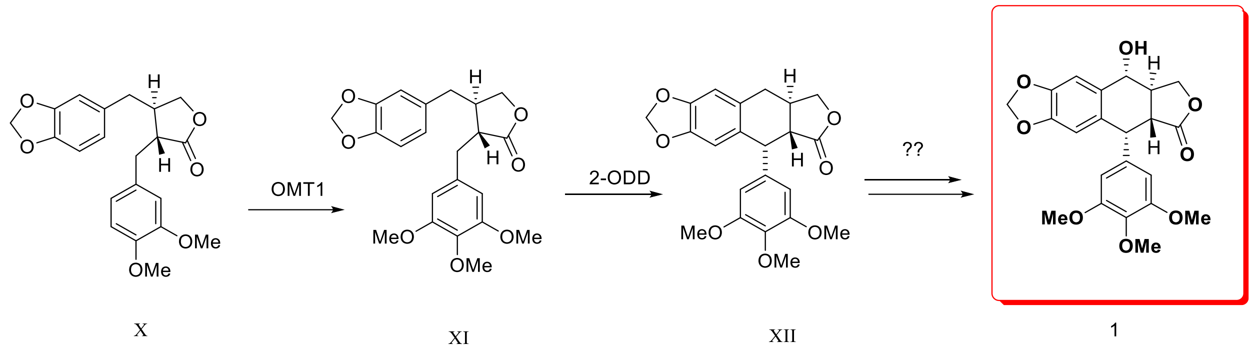

Scheme 4: Biosynthetic pathway from 5'-desmethoxy-yatein X to **1**.

1.8 Structure-activity relationships

Almost all naturally occurring **1** derivatives are accompanied by high systematic toxicity, drug resistance, and low bioavailability. Structurally different **1** derivatives exhibit various antitumor mechanisms based on the motifs they are composed of and cause only mild side effects. The most common derivation is at the 7 position and represents either substitution of hydrogen attached to the oxygen or total interchange of the whole hydroxy group, however, a lot of different modification positions were explored and reported. Further, it was also proved that free rotation of the E-ring is necessary for antitumor activity.

1.8.1 Ring A modifications [21]

Ring A plays a major role in the selection of the mechanism of action and the extent of bioactivity. Opened ring A forming 4,5-dihydroxy compound showed significant activity in inhibition of topoisomerase II corresponding to an approximately 2-fold increase in potency than the etoposide molecule (see fig. 12). It was concluded that 4 and 5 hydroxy functions are as important as 7 hydroxy functions in interaction with enzymes. Protection of those hydroxy functions supported this claim, yielding almost zero bioactivity in the inhibition of topoisomerase II. Protecting hydroxyl groups with variously space-consuming protection groups showed that less bulky substitutions on 4 and 5 had higher bioactivities compared to the ones with more bulky ones. The observed effect can be elucidated with different rates of uptake into the cells, although naturally occurring compounds such as Justicidin B or Diphyllin (see fig. 4) are analogs of **1** with disconnected ring A, and those compounds were reported to be even more bioactive than plain **1** at some cell lines. The exchange of the dihydroxy system for phenylenediamine forming phenazine unit in podophenazine (see fig. 12) showed an entirely different mechanism of action which supports the claim that the A ring is responsible for the mechanism selection.

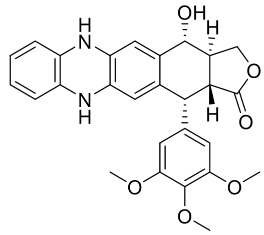

Podophenazine

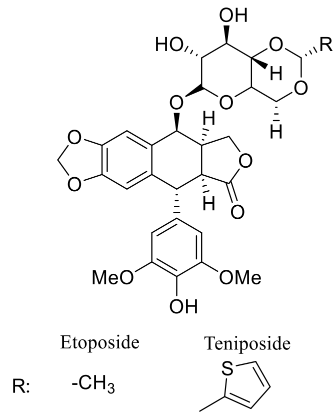

Figure 12: Podophenazine, Etoposide and Teniposide structure.

1.8.2 Ring C modifications

Justicia procumbens plant contains two analogs of **1** that contain an aromatized C-ring. Significant inhibitory activity *in vivo* against P-388 lymphocytic leukemia growth in BDFj male mice (T/C=150% at 50 mg/kg/day) was observed, as well as *in vitro* cytotoxicity in the 9-KB (human nasopharyngeal carcinoma) (ED_{50} < 1.0 µg/mL each) cell culture assay [22]. Aromatization of the C-ring withdraws any topoisomerase II inhibitory activity[23]. Withdrawal is probably caused by dislocation of axially attached D-ring which is essential for bioactivity. The most important modification on the C-ring is a substitution of the hydroxyl group at position 7. Free 7 hydroxy function is essential for DNA strand break activity. All derivatives methylated at the hydroxy group exhibited zero activity [24]. However, Apopicropodophyllotoxin (see fig. 11) was reported to have high cytotoxic activity and showed many-times stronger antimitotic activity than **1**. The positive antimitotic activities of delactonized products indicated that the lactone ring was not needed for antimitotic activity in podophyllotoxin-like compounds. Only 7 hydroxy substitutions were accompanied by cytotoxic properties.

1.8.3 C7-O modifications[25]

Many ether substituents have been incorporated for the purpose of lowering toxicity while maintaining or enhancing activity. The introduction of aminoalkoxy substitution to the 7 position increased both topoisomerase II inhibitory activity and cytotoxic properties of the compound. The ester group can be an important factor for antileukemic and cytotoxic properties, so Lee and co-workers synthesized **1** esters and examined their activities with no major increase detected, but the complete loss of activity seen at most of the compounds. Recently López-Pérez et al. extended a study on esters but introduced linear or aromatic acyl moieties. This modification has either no effect on the resulting activity or even decreasing effect which corresponds with Lee's results. It also indicates that the cytotoxic activity is not primarily due to a lipophilic factor and the precise spatial arrangement of a bulky moiety may contribute to additional nonpolar interactions that can enhance binding to the target site. Compound with N-methyl-N-azidopropylcarbamate group displayed potent cytotoxicity against the L-1210 cell line (IC_{50}, 0.038 μM compared with 0.83 μM for Etoposide) and proved to be a more potent topoisomerase II poison than Etoposide. Kamal et al. also prepared a series of new 4β-carbamoyl-**1** analogs and found higher growth-inhibition activity for 11 different cancer cell lines.

Long-chain fatty acids have recently shown a high impact in terms of cytotoxic properties. Mustafa et al. prepared a series of **1** conjugate with various C10-C20 unusual fatty acids. Serie was tested in vitro for cytotoxic properties against a panel of human cancer cell lines including HL-60 and all of them showed significant cytotoxic properties in all tumor cell lines. IC_{50} of compounds was in the range of 0.07 μM for HL-60 cells to 0.4 μM for KB cells. Interestingly, they did not affect the growth of noncancerous mammalian VERO cells up to the highest concentration (15 μM) used in the assay, demonstrating promising selectivity toward tumor cells.

1.8.4 C7-N modifications

Nitrogen-containing substituents carry an important role in the structure optimization of **1**. Many structures were found to have higher cytotoxicity potency than etoposide. The problem is often basal drug resistance profiles of compounds. Even though many were found to be more potent than etoposide none of them reached clinical status. Even the simplest 7α and 7β alkylamino derivatives did enhance the ability of topoisomerase II inhibition and cellular protein-linked DNA strand breakage. Most potent were found to be 7α isomers, which indicates that the 7 relative configuration is important in determining the inhibitory potency. Various arylamines were introduced into the structure and most of the 7-β arylamines were as much or more potent than etoposide in topoisomerase II inhibition and cellular protein–DNA complex formation assays. The best values were measured for the derivative with *p*-nitrobenzylamin that showed 10-fold higher topoisomerase II inhibitory activity and caused 2-3 times more protein–DNA complex formation than Etoposide (see fig. 13). The compound also caused G2/M phase arrest and could also induce cell death by stimulating tyrosine phosphatase activity and apoptotic DNA formation.

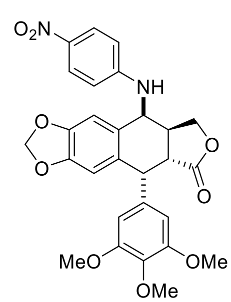

*Figure 13: Structure of **1** substituted with p-nitrobenzylamine on C-7.*

The compound had a great pharmacokinetic profile as well as good stability and bioavailability. This compound reached clinical trials but unfortunately didn't acquire clinical status[26].

1.8.5 Ring D modifications

Picropodophylotoxin (see fig. 14) lacks inhibitory effects on microtubules and cytotoxicity, also does not have an inhibitory effect on topoisomerase II and tubulin and consequently does not cause DNA strand breaks. It is a selective and very effective inhibitor of insulin-like growth factor-1 receptor, which is important for the proliferation of malignant cells. In the presence of a weak base, **1** easily epimerizes to the picropodophyllotoxin and therefore loses most of its properties [27].

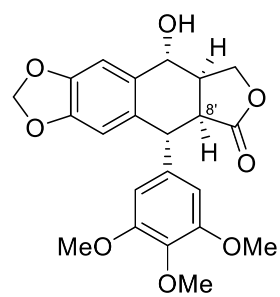

Picropodophyllotoxin

Figure 14: Structure of Picropodophyllotoxin.

1.9 Approved drugs

1.9.1 Etoposide [28]

Etoposide (also commonly known as VP-16) is a mitotic inhibitor that is used in the treatment of neoplastic diseases. Etoposide is epi-podophyllotoxin with a free 5' hydroxy group and glycosylated 7 hydroxy group (see fig. 4). The mechanism of action of a drug is dependent on the concentration. In the case of high concentrations (10 mg/mL or more), lysis of cells entering mitosis is observed. At low concentrations (0.3 to 10 mg/mL), cells are inhibited from entering prophase. The drug does not interfere with microtubule assembly. The main purpose of the drug is to influence topoisomerase II or the formation of ROS species causing DNA strand breaks. The half-life of the drug is approx. 1.5 hours, and it does not accumulate in the plasma. It is highly protein bound (97% bound in plasma proteins). The excretion is 60% over the urine, by which 45% was excreted as Etoposide. Fecal recovery was 15%. There is no evidence for a first-pass effect. The drug is mainly indicated for refractory Testicular tumors and small-cell lung cancer.

1.9.2 Teniposide [18]

Teniposide is structurally very similar to Etoposide with a 2-thienyl group attached to the glycoside moiety (see fig. 4). Teniposide is a phase-specific cytotoxic drug, acting in the late S or early G2 phase of the cell cycle. Teniposide prevents cell mitosis by blocking single and double-stranded DNA breaks and causes cross-linking between protein and DNA. The mechanism of action is similar to the Etoposide inhibition of the Topoisomerase II enzyme. Decomposition half-time is 5 hours and secretion is similar to Etoposide. It is mostly indicated for Refractory Childhood Acute Lymphoblastic Leukaemia.

1.9.3 Podofilox

Podophyllox is a pharmaceutical agent composed of **1** as an active ingredient. Podofilox is a topical antimitotic drug utilized in the treatment of genital warts caused by HPV. The drug acts by binding to microtubules, which prevents cell division and growth, ultimately leading to the regression of warts. The therapeutic efficacy of Podofilox has been established in several clinical trials, demonstrating a favourable response rate with limited systemic toxicity. However, there are potential side effects associated with its use, such as local irritation, itching, and burning. Furthermore, given the potential for teratogenicity, Podofilox is contraindicated in pregnancy. Overall, Podofilox is a well-tolerated and effective treatment option for genital warts, but its administration should be conducted under the supervision of a healthcare provider.

1.10 Known synthetic approaches to Podophyllotoxin.

Many approaches leading to the **1** or its derivatives were published. Most of them are well-reviewed[3,29,30] In a publication from 2008, Linker et. al. presented a novel methodology for the synthesis of epi-podophyllotoxin, which is most probably going to be product of our synthesis as well. It lead to product similar to etoposide and teniposide, which are potent antineoplastic agents.

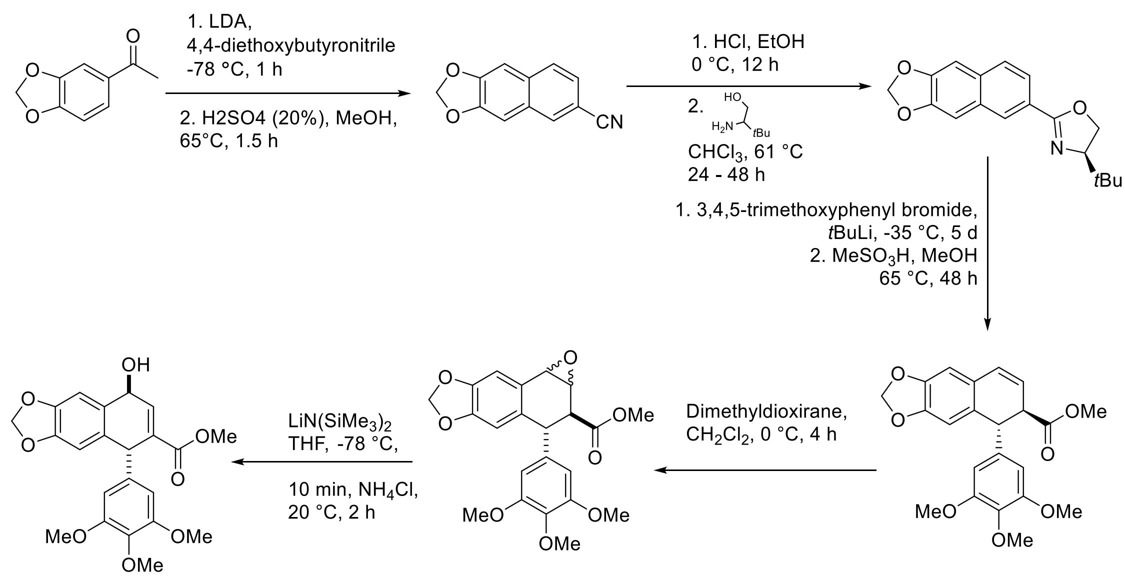

Scheme 5: Linkers total synthesis of epipodophyllotoxin.

The key-step in this synthesis involves the dearomatization of the naphtalenic system, which was achieved through an annelating approach of piperonal into the desired three-cyclic compound, which served as the precursor for the subsequent transformation steps leading to **1**. Linker and co-workers employed a method for introducing oxazoline, which was previously developed by A. I. Meyers in 2009, to transform the nitrile moiety into an oxazoline ring. The synthetic route involved the hydrolysis of the nitrile group to the corresponding carboxylic acid using hydrochloric acid in ethanol and that was followed by treatment with a 2-amino-3,3-dimethylbutanol, which underwent cyclization to form the desired oxazoline ring. The incorporation of an oxazoline group has been demonstrated to be an effective strategy for facilitating the dearomatization of the naphtholic system and subsequent substitution at position 7. Specifically, oxazoline acts as an electron-withdrawing group, which enhances the reactivity of the aromatic system and enables more facile substitution. In this step, 3,4,5-trimethoxyphenyl lithium was utilized to attach to the position 7', whereas oxazoline was then subjected to acidic treatment to promote hydrolysis to a tert-butyl ester. The next step in the reaction was utilizing a double bond at 7,8 position using stereoselective epoxidation with an epoxide ring formation. This ring can be opened leaving the hydroxy group in the correct configuration. Hydroxyl at position 7 was attached to the molecule utilizing 8-8' double bond formed by previous step.

1.11 Synthetic Methodology

1.11.1 Olefin Metathesis

Olefin metathesis was similarly to many technological discoveries and inventions discovered by accident. As part of ongoing research that ended with the invention with the name of Ziegler-Natta catalysis, Karl

Waldemar Ziegler converted ethylene into 1-butene[31]. Olefin metathesis is therefore a reaction recruiting metal catalysts that can attach or detach molecule synthons via their double or triple bonds between carbon atoms. Olefin metathesis can be divided into two types depending on if the reaction mechanism closes a ring - RCM or if the reaction proceeds intermolecularly - CM. This enables one to construct a wide range of cyclic compounds including macrocycles, heterocycles, or natural products.

The reaction is catalyzed by metal carbenes, which are generated *in situ* from metal alkylidenes. Research on these alkylidenes took already a long journey that awarded some scientists Nobel prizes, including Robert H. Grubbs, who explored various catalysts, many of which are named after him.

Alkylidene metal initiates in reaction as a first step of mechanism. Alkene inserts itself to the carbon-metal double bond, forming a metallacyclobutane ring composed of catalyst and substrate. Complex drops ethylene and forms a substrate connected via double bond to the metal. Therefore, this particle acts as catalyst and can include another double bond forming metallacyclobutane. Cleavage of fused product from catalyst complex leaves two molecules interconnected via their double bond system.

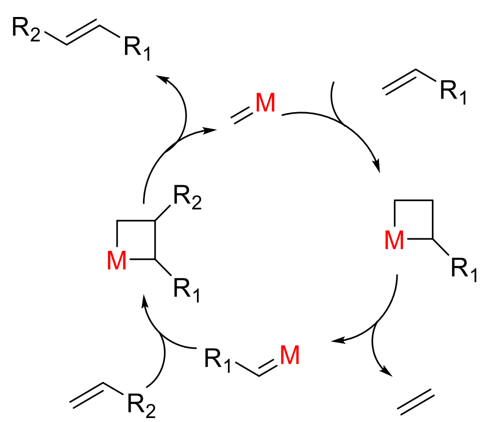

Scheme 6: Mechanism of olefin cross-metathesis.

In the case of ring-closing metathesis, where both double-bond systems are in the same molecule, no side products can be expected. In the case of cross-metathesis, statistical proportions of various parts can be expected (Molecule 1 – Molecule 1, Molecule 1 – Molecule 2, Molecule 2 – Molecule 2).

1.11.2 Conjugate addition

Conjugate addition is a special case of nucleophilic addition to a system of conjugated double bonds. Nucleophiles of various types attack the α,β-unsaturated carbonyl system in the 1,4-manner instead of regular 1,2-addition. This reaction forms a carbon-carbon bond in close proximity to the electrophilic carbonyl.

The reaction mechanism proceeds through the formation of nucleophile, which can be any type of organometallics such as cuprate, organolithium, or *in situ* generated enolate. The nucleophilic attack results in the formation of a new bond between the nucleophile and the β-carbon of the α,β-unsaturated carbonyl compound. This breaks the π bond between the α- and β-carbons, generating a negatively charged intermediate. Negatively charged intermediate can be easily quenched with protic solvent resulting in desired product.

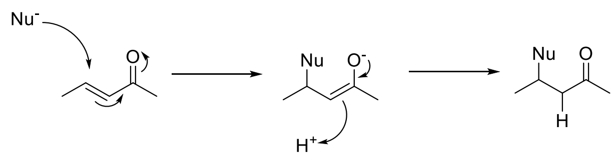

Scheme 7: Mechanism of conjugate addition quenched by protic solvent.

Conjugate additions can be classified into several types depending on the Nucleophile and electrophile e.g. Michael addition is a reaction between Michael donor (enolate) and Michael acceptor (α,β-unsaturated carbonyl). This method is a classical approach for the preparation of β-substituted carbonyls. It can also proceed diastereoselectively and enantioselectively as many asymmetric variants exists.

An electron-poor double-bond system is desirable. Aldehydes and ketones are among the most reactive species. Carboxylic acids cannot be successfully used, as acidic hydrogen quenches most of the nucleophiles used in conjugate additions, and regular carboxylic acid derivatives can be too deactivated. Diastereo- and enantioselectivity can be challenging.

2 Aims of the work

Derivatives of **1** were acknowledged as potent drugs against various neoplastic illnesses. The main purpose of this study is to design an enantioselective method leading to the total synthesis of the natural product **1** or some of its derivative. We have established several partial goals, which follows:

1. Optimize the conjugate addition without electrophile capture of **2** and **3** (see scheme 8).
2. Optimize the deprotonation of **4** and the addition of electrophile.
3. Optimize the conjugate addition with electrophile capture of **2** and **3** as one of a key step of the reaction scheme.
4. Optimize elimination leading to general methylenation of **4.**
5. Optimize the olefin metathesis reaction for low- and large-scale production of **8** as one of a key step of the reaction scheme.
6. Optimize the conjugate addition of **8.**

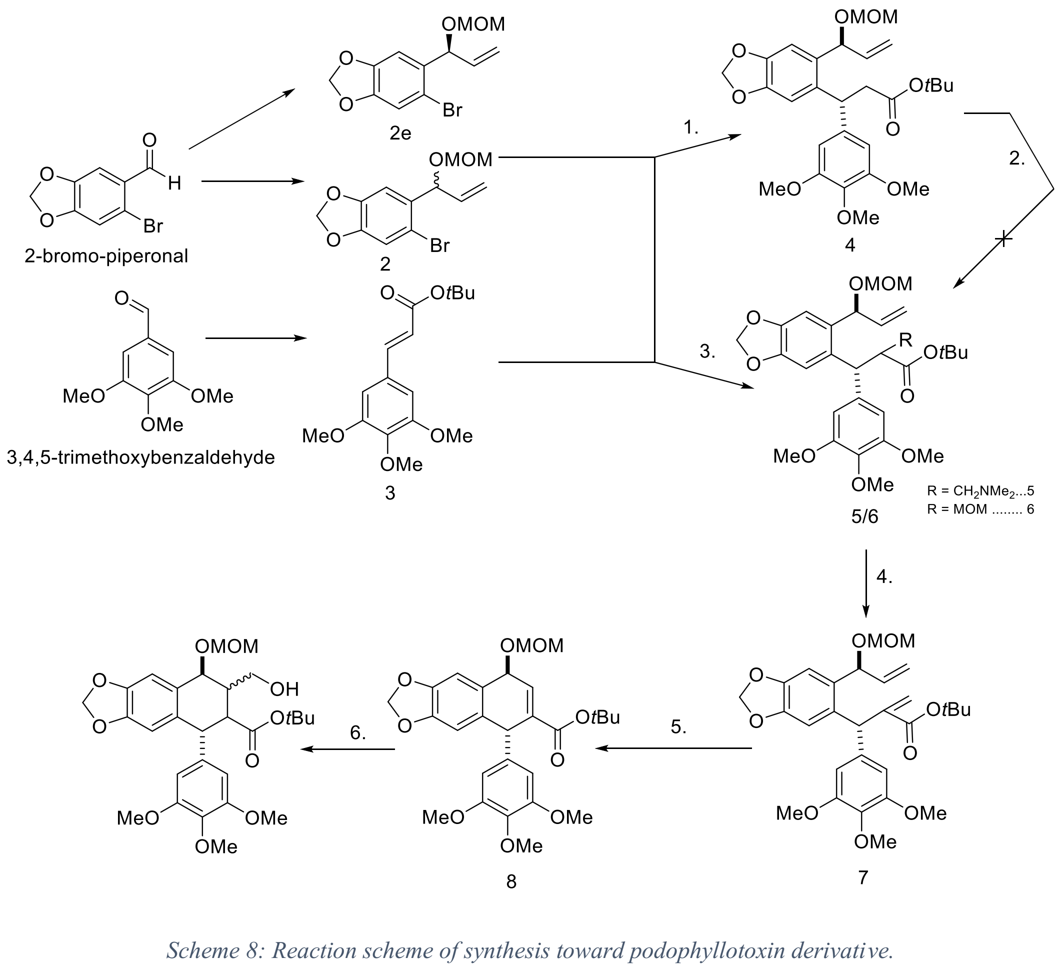

Scheme 8: Reaction scheme of synthesis toward podophyllotoxin derivative.

3 Experimental part

*3.1 (S)-1-(6-Bromobenzo[d][1,3]dioxol-5-yl)prop-2-en-1-ol (**2**)*

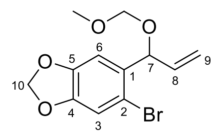

2

Preparation

2-Bromopiperonal (802 mg, 3.5 mmol) was added to a dried 100mL round bottom flask equipped with a magnetic stirring bar and dissolved in 20 mL of dry THF. The solution was cooled to 0 °C by an ice bath and vinylmagnesiumchloride (3.85 mL, 3.85 mmol, 1.1 equiv.) was added dropwise. After 5 min, the reaction was heated to rt. TLC was used to monitor the reaction progress, and full conversion was achieved as the temperature reached room temperature. DIPEA (1.34 mL, 7.7 mmol), TBAI (65 mg, 0.175 mmol), and MOMCl (530 µL, 7 mmol, 2 equiv.) were subsequently added to the reaction mixture, and the reaction was stirred overnight. TLC was used to confirm the completion of the reaction. The reaction mixture was quenched with a saturated $NaHCO_3$ solution (50 mL). The mixture was transferred to a separatory funnel, diluted with an additional 50 mL of $NaHCO_3$, and extracted with petroleum ether (3x50 mL). The combined organic layers were dried with saturated brine, anhydrous magnesium sulfate, and evaporated under vacuum to give a slightly yellowish-gelly compound. The bromide was purified by column chromatography (SiO_2, Et_2O: Hexane 1:4) to yield 0.97 g (92%) of pure product **2**.

Rf: = 0.3 (1:6 EtOAc:Hex); **IR** $\tilde{\nu}$ [cm^{-1}] (m/z , rel. intensity): (3657-3085, w), (2980, w), (2898, w), (1502, w), (1474, s), (1408, w), (1389, w), (1359, w), (1234, m), (1115, w), (1038, m),(987, w), (932, w), (870, w), (840, w), (798, w); **MS** (ESI+) (m/z , rel. intensity [%]): (325/323, 11/12, $[M + Na]^+$), (241/239, 11/12, $[M + H – MeOH – CH2O]^+$), (215/213, 18/18, $[M + H – MeOH – CH2O – C2H2]^+$), (188, 20), (160, 100, $[M + H – MeOH – CH2O –Br]^+$), (130, 26); **HRMS** (ESI+) *m/z* $[M+Na^+]$ calcd for $C_{12}H_{13}O_4BrNa$: 322.9889 found: 322.9892; **^{1}H NMR** (400 MHz, $CDCl_3$): δ = 6.98 (s, 1H, H-3/6), 6.97 (s, 1H, H-3/6), 5.97 (m, 2H, H-10), 5.85 (ddd, J = 17.2, 10.35, 5.99 Hz, 1H, H-8), 5.48 (dt, J = 6.02, 1.34 Hz, 1H, H-7), 5.36 (dt, J = 17.16, 1.44 Hz, 1H, H-9a), 5.23 (dt, J = 10.40, 1.44 Hz, 1H, H-9b), 4.70 (d, J = 6.6 Hz, 1H, C7-$OC\underline{\mathit{H}}_aH_bOCH_3$), 4.60 (d, J = 6.66 Hz, 1H, C7-$OCH_a\underline{\mathit{H}_b}OCH_3$), 3.41 (s, 3H, C7-$OCH_2OC\underline{\mathit{H}_3}$); **^{13}C NMR**

(400 MHz, $CDCl_3$): δ = 147.8 (s, C-4/5), 147.9 (s, C-4/5), 136.8 (d, C-8), 133.3 (s, C-1), 116.5 (t, C-9), 113.4 (s, C-2), 112.4 (s, C-3/6), 108.1 (s, C-3/6), 101.8 (t, C-10), 94.0 (t, C7-O$\underline{C}H_2OCH_3$), 76.6 (d, C-7), 55.7 (q, C- C7-$OCH_2O\underline{C}H_3$).

*3.2 trans-3,4,5-trimethoxybenzyl-tBu-prop-2-enoate (**3**)*

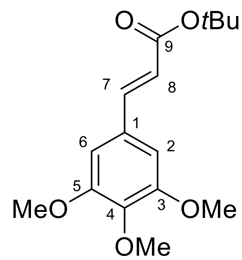

3

Preparation

t-Butyl-diethylphosphoacetate (7.94 g, 31.5 mmol) was added to a dried 500mL round bottomed flask equipped with a magnetic stirring bar and dissolved in 150 mL of dry THF. *t*-BuOK (7.06 g, 63 mmol, 2 equiv.) was dissolved in THF and injected to the flask. The solution was cooled to 0 °C in a water-ice bath and 3,4,5-trimethoxybenzaldehyde (6.18 g, 31.5 mmol) was added dropwise dissolved in 2 mL of dry THF. The reaction was stirred overnight. NMR analysis showed the absence of starting material, so the reaction was quenched by saturated $NaHCO_3$ solution (50 mL) and transferred into a separation funnel. The reaction mixture was extracted with deionized water (2 x 50 mL) and brine solution (1 x 50 mL). The combined organic layers were dried with anhydrous sodium sulfate and evaporated *in vacuo*. The product was filtered over a small silica column, yielding 3.14 g of pure product (33.8%).

R_f = 0.65 (EtOAc:Hex 1:3); **M.p.** = 76-77 °C**; IR** $\tilde{\nu}$ [cm^{-1}] (m/z , rel. intensity): (3022-2850, w), (2826, w), (1696, m), (1582, m), (1504, m), (1467, w), (1457, w), (1448, m), (1420, m), (1312, m), (1276, m), (1247, m), (1144, s), (1121, vs), (1009, m), (995, m), (846, s), (834, w), (742, w), (622, w); **MS** (ESI+) (m/z, rel. intensity [%]): **(**411.0, 25), (323.0, 10), (239, 13), (215, 20), (188, 21), (161.1, 10), (160.1, 100), (130, 25), (102, 73); **HRMS** (ESI+) m/z: calcd for $C_{15}H_{21}O_5Na$: 317.1359 found: 317.1359 ($[M+Na]^+$); **^{1}H NMR** (400 MHz, $CDCl_3$): δ = 7.49 (d, J = 15.87 Hz, 1H, H-7), 6.73 (s, 2H, H-2,6), 6.27 (d, J = 15.84 Hz, 1H, H-8), 3,88 (s, 9H, Ar-^{m,p}OC$\underline{H_3}$), 1.53(s, 9H, *t*Bu); **^{13}C NMR** (400 MHz, $CDCl_3$): δ = 166.7 (s, C-9), 153.8 (s, C-4), 143. (d, C-7), 140.26 (s, C-1), 130.6 (d, 2C, C-3, C-5), 119.9 (d, C-8), 104.8 (d, 2C, C-2, C-6), 80.9 (s, $\underline{C}(CH_3)_3$), 61.3 (q, Ar-^{p}O-*<u>Me</u>*), 56.5 (q, Ar-^{m}O-*<u>Me</u>*), 29.3 (q, $C(\underline{C}H_3)_3$).

*3.3 (S)-1-(6-Bromobenzo[d][1,3]dioxol-5-yl)prop-2-en-1-ol (**2e**)*

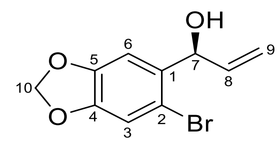

Preparation

To degas reaction solvent, 10 mL of methanol was combined with 2 drops of water, and the mixture was added to the large Schlenk flask. Five cycles of reducing pressure to the boiling point of MeOH using a high vacuum pump, allowing for a few seconds of boiling, and then injecting nitrogen to relieve pressure, were performed. Another Schlenk flask was vacuum-dried and filled with a nitrogen atmosphere. Copper fluoride $CuF_2 \cdot H_2O$ (3 mg, 0.025 mmol, 0.037 equiv.) and (R)-DTBM-SEGPHOS (50 mg, 0.042 mmol, 0.063 equiv.) were added to the flask. The system was subjected to vacuum for approx. 2 min and then filled with nitrogen. Degassed MeOH was added to the Schlenk flask leading to the formation of a white precipitate, which eventually changed color to the slight purple hue. The reaction was heated to reflux for 30 min and dry THF (0.4 mL) was added to dissolve the white precipitate. No blue copper salt residue was detected. The reaction was refluxed for another 20 min, after which a reaction mixture was evaporated. The same mixture of solvents was added 2 more times and the process was repeated. Dry toluene was added (0.5 mL) completely dissolving the reaction mixture. The toluene was evaporated under a vacuum to remove solvent residues and humidity, and the process was repeated one more time. 6-Bromo-piperonal (153 mg, 0.67 mmol) was added. The flask was subjected to vacuum and then filled with nitrogen. DMF (1 mL) and trimetoxyvinylsilane (205 µL, 1.34 mmol, 2 equiv.) were added and the reaction mixture was stirred for 30-40 min after which NMR measurement was performed. Measurement gave full conversion so the reaction was quenched with water. The crude reaction mixture was transferred to a tall beaker and the flask was flushed with water and EtOH mixture approx. 1:1. to ensure full transfer of the mixture. A 10% KOH solution (5 mL) was added to the mixture heated to 50 °C and stirred for 20 min. The mixture was extracted with 40 mL of water and 2 x 30 mL of Et_2O:PE mixture in a ratio of 1:1. The aqueous phase was reextracted with an additional 20 mL of Et_2O. The combined organic layers were reextracted with brine and filtered over anhydrous sodium sulfate. Residue recrystallized in 10% EtOAc:PE mixture. The recrystallization process yielded 143 mg of pure product corresponding to 93% yield and enantiomeric excess ee of 94%. The crystals were suitable for X-ray analysis, which was used to establish absolute configuration as (*S*)-**2e.**

Rf: = 0.3 (EtOAc:Hex 1:6); **IR** $\tilde{\nu}$ [cm^{-1}] (m/z , rel. intensity): (3658-3085, b), (2980, 0. w), (2899, w), (1502, m), (1475, vs), (1408, w), (1390, w), (1359, w), (1234, s), (1115, w), (1039, s), (987, w), (933, m), (870, w), (840, w), (799, w); **MS** (APCI+) (m/z , rel. intensity [%])**:** (483.2, 15), (241.0, 90), (239.0, 100), (217.4, 10), (209.0, 14), (171.1, 30); **HRMS** (APCI+) m/z: calcd for $C_{16}H_{22}O_5Na$: 317.1359 found: 317.1359; ^{1}**H NMR** (401 MHz, CDCl3): δ = 7.01 (s, 1H, H-3/6), 6.98 (s, 1H, H-3/6), 5.98 (dd, J = 1.37, 4.45 Hz, 2H, H-10), 5.97 (ddd, J = 15.9, 10.5, 5.4 Hz 1H, H-8), 5.54 (ddd, J = 5.07, 3.21, 1.49 Hz, 1H, H-7), 5.40 (ddd, J = 17.2, 1.5, 1.5 Hz, 1H, H-9a), 5.22 (ddd, J = 10.4, 1.4, 1.4 Hz, 1H, H-9b), 2.02 (s, 1H, C7-O*H*); ^{13}**C NMR** (401 MHz, CDCl3): δ = 179.9 (s, C-4/5), 148.0 (s, C-4/5), 138.5 (d, C-8), 135.0 (s, C-1), 115.5 (t, C-9), 113.1 (s, C-2), 112.7 (d, C-3/6), 107.9 (d, C-3/6), 101.9 (t, C-10), 73.5 (d, C-7).

3.4 tert-Butyl (R)-3-(6-{(S)-1-[(methyloxy)methoxy]allyl}benzo[d][1,3]dioxol-5-yl)-3-(3,4,5-trimethoxyphenyl)propanoate (**4**)*

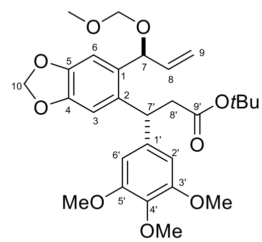

4

Preparation

Bromide **2** and Cinnamate **3** were 3x dissolved in benzene and evaporated *in vacuo* for a removal of residual humidity. Compounds were dried for 10 min at the vacuum pump. Schlenk flask was fitted with a magnetic stirrer and dried with a heat gun. A nitrogen atmosphere was introduced after couple min of drying. Dry toluene (2 mL) was injected into the flask and bromide **2** (45 mg, 0.015 mmol) was weighted in a syringe, in which it was dissolved and washed into the reaction mixture in dry toluene. The apparatus was cooled by a dry ice-acetone cooling bath to -78 °C. Dry TMEDA (150 µL, 1.5 mmol) and BuLi (87 µL, 1.6M, 0.14 mmol) were added dropwise and the reaction was stirred for 10 min at -78 °C, and then 10 min slightly pulled out of bath. Cinnamate **3** (19 mg, 0.1 mmol) was added dissolved in a syringe and the reaction was stirred for 3-4 hours during what the reaction was gradually heated to rt. The reaction mixture was quenched with wet Et_2O and stirred overnight at rt. The reaction mixture was then filtered over a silica column, eluted with Et_2O and evaporated *in vacuo*. Ester **4** was isolated by flash chromatography which obtained a single diastereomer. The reaction yielded 26 mg of pure product (62%) as 5.5:1 diastereomer mixture.

Rf: = 0.4 (EtOAc:Hex 1:3)**; IR** $\tilde{\nu}$[cm^{-1}] (m/z , rel. intensity): (3057-2887, b), (2838, w), (1712, w), (1628, w), (1588, m), (1504, m), (1482, w), (1461, w), (1419, w), (1367, w), (1328, m), (1253, m), (1234, m), (1125, vs), (1028, s), (933, m), (849, m), (733, s), (701, w); **MS** (ESI+) (m/z , rel. intensity [%]): (669, 5), (540, 20), (539, 65), (535, 10), (400, 25), (399, 100), (340, 40), (339, 92); **HRMS** (ESI+) m/z: calcd for $C_{28}H_{36}O_9Na$: 539.2251 found: 539.2249; **^{1}H NMR** (400 MHz, $CDCl_3$)**:** δ = 6.91 (s, 1H, H-3/6), 6.68 (s, 1H, H-3/6), 6.39 (s, 2H, H-2', H-6'), 5.96 – 5.88 (m, 2H, H-10a, H-10b), 5.79 (ddd, *J* = 16.8, 10.7, 6.0 Hz, 1H, H-8), 5.47 (dt, *J* = 6.1, 1.4 Hz, 1H, H-7), 5.16 – 5.01 (m, 2H, H-9), 4.77 (dd, *J* = 8.8, 7.2 Hz, 1H, H-7'), 4.67 – 4.56 (m, 2H, H-10), 3.78 (s, 9H, Ar-^{m,p}O-*Me*), 3.40 (s, 3H, C7-$OCH_2OC\underline{H}_3$)2.92 – 2.77 (m, 2H, H-8'), 1.33 (s, 9H, $C(C\underline{H}_3)_3$); **^{13}C NMR** (400 MHz, CDCl3): δ = 170.9 (s, C-9'), 153.2 (s, 2C, C-3', C-5'), 147.3 (s, C-4/5), 146.4 (s, C-4/5), 139.4 (s, C-1'), 138.4 (d, C-8), 136.6 (d, C-4'), 135.3 (s, C-2), 131.9 (s, C-1), 116.1 (t, C-9), 108.1 (d, C-3/6), 107.3 (d, C-3/6), 105.1 (d, 2C, C-2', C-6'), 101.2 (t, C-10), 93.6 (t, C7-$O\underline{C}H_2OCH_3$), 80.7 (s, $\underline{C}(CH_3)_3$), 73.7 (d, C-8), 60.9 (q, ^{p}O-*Me*), 56.2 (q, 2C, ^{m}O-*Me*), 55.6 (q, C7-$OCH_2O\underline{C}H_3$), 42.6 (t, C-8'), 42.2 (d, C-7'), 28.1 (q, $C(\underline{C}H_3)_3$).

3.5 tert-Butyl (3R)-2-((dimethylamino)methyl)-3-(6-((S*)-1-(methoxymethoxy)allyl)benzo[d][1,3]dioxol5-yl)-3-(3,4,5-trimethoxyphenyl)propanoate (**5**)*

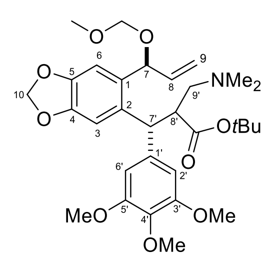

5

Preparation

A 250mL Schlenk flask was heated with a heat gun under vacuum for humidity removal. A nitrogen atmosphere was introduced. Bromide **2** (7.16 g, 23.78 mmol, 1.4 equiv.) was weighted into the flask and placed under vacuum for drying. A flask was filled with a nitrogen atmosphere. Dry toluene was added to the flask and TMEDA (25.5 mL, 33.9 mmol, 2 equiv.) was added dropwise via syringe. The system was cooled to -78 °C and BuLi (16.6 mL, 23.8 mmol, 1.4 equiv.) was added dropwise. The reaction mixture turned bright yellow and was stirred for 15 min. Cinnamate **2** (5.0 g, 16.9 mmol) was dissolved in toluene and added dropwise by syringe. The reaction went from bright yellow to dark orange and back again to bright yellow within 2 min. The reaction was stirred for 2 hours at -78°C. Dry THF (5 mL) was added followed by Eschenmoser's salt (6.3 g, 33.9 mmol, 2 equiv.). The mixture was vigorously stirred, and the reaction temperature was gradually increased to room temperature over the course of 1-2 hours. 6.5 g of the mixture was subjected to column (1 l of 30% Et_2O, then pure ether), which acquired 6 g of product (60%).

R$_f$ = 0.15 (Et_2O); **IR** $\tilde{\nu}$[cm^{-1}] (m/z , rel. intensity): (3078, w), (2974, w), (2865, w), (1726, w), (1588, w), (1505, w), (1484, m), (1367, w), (1233, m), (1125, vs), (1030, vs), (932, m), (846, w); **MS** (ESI+) (m/z, rel. intensity): (574, 1.0, $[M + H]^+$), (512, 0.16, $[M - CH_3OCH_2O]^+$), (456, 0.32, $[M - CH_3OCH_2O - \text{isobutene}]^+$), (339, 0.35); **HRMS** (ESI+) *m/z*: $[M + H]^+$ calcd. for $C_{31}H_{44}O_9N$ 574.3011; found: 574.3008; **^{1}H NMR** (401 MHz, C_6D_6): δ 7.40 (s, 1H, H-3/6), 7.29 (s, 1H, H-3/6), 6.62 (s, 2H, H-2', H-6'), 5.99 (dt, *J* = 5.8, 1.4 Hz, 1H, H-7), 5.81 (ddd, *J* = 17.1, 10.3, 5.8 Hz, 1H, H-8), 5.37 (d, *J* = 1.3 Hz, 1H, C4-OCH_aH$_b$O), 5.28 (d, *J* = 1.3 Hz, 1H, C4-OCH$_a\mathit{H}_b$O), 5.21 (dt, *J* = 17.2, 1.6 Hz, 1H, H-9a), 4.97- 4.90 (m, 2H, H-9b, C7-OCH_aH$_b$OCH$_3$), 4.74 (d, *J* = 6.5 Hz, 1H, C7-OCH$_a\mathit{H}_b$OCH$_3$), 4.61 (d, *J* = 11.4 Hz, 1H, H-7'), 3.78 (s, 3H, C4'-OCH_3), 3.57-3.50 (m, 1H, H-8'), 3.43 (s, 3H, C7-OCH$_2$OCH_3), 3.36 (s, 6H, C3'-OCH_3, C5'-OCH_3), 2.98 (t, *J* = 11.5 Hz, 1H, H-10'a), 2.32-2.23 (m, 1H, H-10'b), 2.12 (s, 6H, N(CH_3)$_2$), 1.32 (s, 9H, OC(CH_3)$_3$); **^{13}C NMR** (401 MHz, C_6D_6): δ 173.6 (s, *C*OO*t*-Bu), 154.2 (s, 2C, C-3', C-5'), 147.5 (s, C-4/5), 147.0 (s, C-4/5), 139.5 (d, C-8), 138.3 (s, C-1'), 138.2 (s, C-4'), 134.6 (s, C-1/2), 133.8 (s, C-1/2), 115.9 (t, C-9), 108.6 (d, C-3/6), 108.0 (d, C-3/6), 106.3 (d, 2C, C-2', C-6'), 101.1 (t, C-10), 94.3 (t, C7-O*C*H$_2$OCH$_3$), 80.0 (s, O*C*(CH$_3$)$_3$), 73.9 (d, C-7), 62.2 (t, C-9'), 60.5 (d, Ar-^{p}O-<u>*Me*</u>), 55.9 (q, 2C, Ar-^{m}O-<u>*Me*</u>), 55.7 (q, C7-OCH$_2$O*C*H$_3$), 50.9 (d, C-8'), 47.5 (d, C-7'), 45.7 (q, 2C, N(*C*H$_3$)$_2$), 28.0 (q, OC(*C*H$_3$)$_3$).

3.6 tert-Butyl (3R)-3-(6-((S*)-1-(methoxymethoxy)allyl)benzo[d][1,3]dioxol-5-yl)-2-(methoxymethyl)-3-(3,4,5-trimethoxyphenyl)propanoate (**6**)*

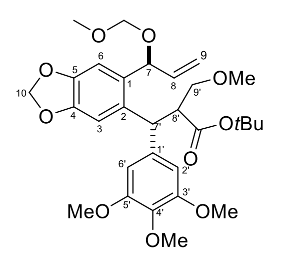

6

Preparation

A Schlenk flask was dried using a heat gun and fitted with a magnetic stirring bar. The flask was purged with nitrogen. Dry THF was injected in the flask and tetramethylpiperidine (TMP) (55 µL, 0.328 mmol) was added. The reaction mixture was cooled to -78 °C with an acetone/dry ice cooling bath. BuLi (180 µL, 1.7M, 0.289 mmol, 1.5 equiv.) was added dropwise and the reaction mixture was stirred for 30 min during which the temperature was gradually increased to 0 °C. The reaction temperature was again cooled to – 78

°C, and compound **3** (100 mg, 0.193 mmol) was added dissolved in THF to the reaction mixture and stirred for 1 hour at this temperature. Methoxymethyl chloride (30 µL, 0.386 mmol, 2 equiv.) was added diluted in 1 mL of dry THF and the reaction temperature was allowed to increase to rt over the course of 30-40 min and quenched with wet Et_2O. The quenched reaction mixture was extracted with 150 mL EtOAc and 150 mL of aqueous NH_4Cl. The aqueous phase was reextracted with 50 mL of EtOAc and the combined organic layers were treated with brine and anhydrous sodium sulfate. Evaporation yielded 100 mg of the product mixture which was subjected to isolation at flash chromatography to yield 50 mg of starting material and 40 mg of clean product (41%) as a 2:1 diastereomeric mix.

R$_f$ = 0.73 (hexane/EA 1:1); **IR** $\tilde{\nu}$[cm^{-1}] (m/z , rel. intensity): (2976, w), (2934, w), (2891, w), (2836, w), (1724, m), (1589, m), (1505, m), (1484, m), (1459, m), (1421, w), (1367, w), (1328, w), (1230, m), (1147, s), (1125, vs), (1030, vs), (910, s), (846, w), (728, vs), (647, w); **MS** (ESI+) (m/z, rel. intensity): (1143, 13, $[2M + Na]^+$), (583, 100, $[M +Na]^+$), (578, 17, $[M + NH_4]^+$), (339, 70); **HRMS** (ESI+) *m/z*: $[M + Na]^+$ calcd. for $C_{30}H_{40}O_{10}Na$ 583.25137; found: 583.25123; **^{1}H NMR** (401 MHz, $CDCl_3$, A major diastereomer, B minor diastereomer): δ 7.04 (s, 1H, H-3/6$_A$), 6.90 (s, 1H, H-3/6$_B$), 6.88 (s, 1H, H-3/6$_A$), 6.83 (s, 1H, H-3/6$_B$), 6.50 (s, 2H, H-2'$_B$), 6.43 (s, 2H, H-2'$_A$), 5.95 (d, *J* = 1.4 Hz, 1H, C4-OC*H*$_a$H$_b$O$_B$), 5.92 (d, *J* = 1.4 Hz, 1H, C4-OC*H*$_a$H$_b$O$_A$), 5.91 (d, *J* = 1.4 Hz, 1H, C4-OCH$_a$*H*$_b$O$_A$), 5.88 (d, *J* = 1.5 Hz, 1H, C4-OCH$_a$*H*$_b$O$_B$), 5.90-5.82 (m, 1H, H-8$_B$), 5.63 (ddd, *J* = 16.8, 10.3, 5.6 Hz, 1H, H-8$_A$), 5.57- 5.52 (m, 2H, H-7$_{AB}$), 5.24-5.17 (m, 2H, H-9$_B$), 5.02-4.93 (m, 2H, H-9$_A$), 4.68 (d, *J* = 6.8 Hz, 1H, C7-OC*H*$_a$H$_b$OCH$_{3B}$), 4.65 (d, *J* = 6.6 Hz, 1H, C7-OC*H*$_a$H$_b$OCH$_{3A}$), 4.61 (d, *J* = 6.6 Hz, 1H, C7- OCH$_a$*H*$_b$OCH$_{3A}$), 4.56 (d, *J* = 6.6 Hz, 1H, C7-OCH$_a$*H*$_b$OCH$_{3B}$), 4.37 (d, *J* = 11.3 Hz, 1H, H-7'$_B$), 4.34 (d, *J* = 10.7 Hz, 1H, H-7'$_A$), 3.79 (s, 6H, Ar-^{m}O-*Me*$_B$), 3.79 (s, 6H, Ar-^{m}O-*Me*$_A$), 3.77 (s, 3H, Ar-^{p}O-*Me*$_A$), 3.75 (s, 3H, Ar-^{p}O-*Me*$_B$), 3.66-3.58 (m, 1H, C8'-C*H*$_a$H$_b$OCH$_{3B}$), 3.55-3.48 (m, 1H, C8'- C*H*$_a$H$_b$OCH$_{3A}$), 3.46 (s, 3H, C7-OCH$_2$OC*H*$_{3A}$), 3.42 (s, 3H, C7-OCH$_2$OC*H*$_{3B}$), 3.35-3.27 (m, 4H, H- 8'$_{AB}$, C8'-CH$_a$*H*$_b$OCH$_{3AB}$), 3.25 (s, 3H, C8'-CH$_2$OC*H*$_{3A}$), 3.24 (s, 3H, C8'-CH$_2$OC*H*$_{3B}$), 1.25 (s, 9H, C(C*H*$_3$)$_{3A}$), 1.23 (s, 9H, C(C*H*$_3$)$_{3B}$); **^{13}C NMR** (101 MHz, $CDCl_3$, A major diastereomer, B minor diastereomer): δ 172.9 (s, *C*OO*t*-Bu$_B$), 172.5 (s, *C*OO*t*-Bu$_A$), 153.2 (s, 2C, C- 3'$_A$, C-5'$_A$), 152.9 (s, 2C, C-3'$_B$, C-5'$_B$), 147.7 (s, C-4/5$_B$), 147.0 (s, C-4/5$_A$), 146.7 (s, C-4/5$_B$), 146.4 (s, C-4/5$_A$), 138.6 (d, C-8$_B$), 138.4 (d, C-8$_A$), 137.8 (s, C-1'$_B$), 137.7 (s, C-1'$_A$), 136.8 (s, C-4'$_A$), 136.7 (s, C-4'$_B$), 133.6 (s, C-2$_B$), 133.5 (s, C-2$_A$), 133.0 (s, C-1$_A$), 132.1 (s, C-1$_B$), 117.0 (t, C-9$_B$), 115.8 (t, C-9$_A$), 108.3 (d, C-3/6$_A$), 107.7 (d, C-3/6$_B$), 107.1 (d, C-3/6$_A$), 106.5 (d, C-3/6$_B$), 105.8 (d, 2C, C- 2'B), 105.4 (d, 2C, C-2'A), 101.3 (t, C4-O*C*H$_2$O$_B$), 101.2 (t, C4-O*C*H$_2$O$_A$), 93.9 (t, C7- O*C*H$_2$OCH$_{3A}$), 93.6 (t, C7-O*C*H$_2$OCH$_{3B}$), 80.78 (s, COO*C*(CH$_3$)$_{3B}$), 80.77 (s, COO*C*(CH$_3$)$_{3A}$), 73.8 (d, C-7$_B$), 73.5 (t, C8'-*C*H$_2$OCH$_{3A}$), 73.2 (t, C8'-*C*H$_2$OCH$_{3B}$), 73.0 (d, C-7$_A$), 61.0 (q, C-4'$_A$), 60.9 (q, C4'-O*C*H$_{3B}$), 59.1 (q, C8'-CH$_2$O*C*H$_{3A}$), 59.0 (q, C8'-CH$_2$O*C*H$_{3B}$), 56.3 (q, 2C, C3'-O*C*H$_{3A}$), 56.2 (q, 2C, C3'-O*C*H$_{3B}$), 55.9 (q, C7-OCH$_2$O*C*H$_{3A}$), 55.8 (q, C7-

OCH_2OCH_{3B}), 52.4 (d, C-8'B), 52.0 (d, C-8'A), 45.4 (d, C-7'A), 44.7 (d, C-7'B), 27.91 (q, *C*(CH_3)$_{3A}$), 27.90 (q, O*C*(CH_3)$_{3B}$).

3.7 tert-Butyl-2-((R)-(6-((S*)-1-(methoxymethoxy)allyl)benzo[d][1,3]dioxol-5-yl)(3,4,5-trimethoxyphenyl)methyl)acrylate (7)*

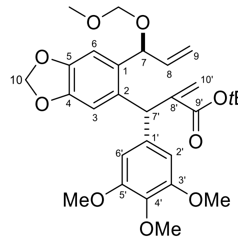

7

Preparation

Amine **4** (800 mg, 1.395 mmol) was dissolved in dry THF (5 mL) in a heat gun dried Schlenk flask. Methyl Iodide (434 µL, 6.9 mmol, 5 equiv.) was added dropwise to the reaction mixture, and the reaction was stirred for approx. two hours at rt. The reaction mixture was evaporated *in vacuo*. The residue was dissolved in a 3 mL mixture of dry THF/*t*BuOH in a 1:1 ratio. Subsequently, *t*BuOK (157 mg, 1.4 mmol, 1.0 equiv.) dissolved in 0.5 mL of dry THF/tBuOH mixture was added to the reaction and then stirred for 10 min. More *t*BuOK (78 mg, 0.7 mmol, 0.5 eq.) was added and the reaction was stirred for additional 30 min, after which it was quenched with water. The reaction mixture was filtered over silica gel with 150 mL of Et_2O. The product was isolated by flash chromatography and acquired 660 mg of pure product (83%).

R_f 0.50 (EtOAc:Hex 1:3); **IR** $\tilde{\nu}$[cm^{-1}] (m/z , rel. intensity): (2935-2837, b), (1705, m), (1502, w), (1483, m), (1459, m), (1302, s), (1231, s), (1142, vs), (1123, s), (1035, m), (1007, s), (934, m), (848, w), (736, w); **MS** (ESI+) (m/z , rel. intensity): (1143.5, 15), (584.3, 30), (583.3, 100), (578.3, 18), (443.2, 22), (340.3, 15), (339.1, 70); **HRMS** (ESI+) m/z: $[M+Na]^+$ calcd for $C_{29}H_{36}O_9Na$: 551.2251; found: 551.2252; **^{1}H NMR** (400 MHz, $CDCl_3$): δ =7.01 (s, 1H, H-3/6), 6.45 (s, 1H, H-3/6), 6.31 (t, J = 1.2 Hz, 1H, H-10'a), 6.29 (s, 2H, H-2',H-6'), 5.92 (dd, J = 7.1, 1.4 Hz, 2H, H-10), 5.79 (ddd, J = 17.0, 10.2, 6.7 Hz, 1H, H-8), 5.46 (d, J = 1.4 Hz, 1H, H-7'), 5.24 (dt, J = 6.7, 1.2 Hz, 1H, H-7), 5.18 – 5.09 (m, 2H, H-10'a, H-10'b), 4.65 (d, J = 6.48 Hz, 1H, C7-OC$\underline{H}_a$H$_b$OCH$_3$) – 4.57 (d, J = 6.54 1H, C7-OCH$_a\underline{H}_b$O CH$_3$), 3.82 (s, 3H, Ar-^{p}O-Me), 3.76 (s, 6H, Ar-^{m}O-Me), 3.35 (s, 3H, C7-OCH$_2$OC$\underline{H}_3$), 1.37 (s, 9H, t-Bu); **^{13}C NMR** (400 MHz, $CDCl_3$): δ = 166.0 (s, C-9'), 153.2 (s, 2C, C-3'), 146.8 (s, C-4/5), 146.4 (s, C-4/5), 145.1 (s, C-8'), 138.1 (d, C-8), 137.5 (s, C-1'), 136.6 (s, C-4'), 133.3 (s, C-2), 132.4 (s, C-1), 126.4 (t, C-10'), 116.2 (t, C-9), 109.1 (d, C-

3/6), 107.7 (d, C-3/6), 106.1 (d, 2C, C-2', C6'), 101.1 (t, C-10), 93.5 (t, C7-O<u>C</u>H_2OCH_3), 80.9 (s, <u>*C*</u>(CH_3)$_3$), 74.1 (d, C-7), 60.9 (q, Ar-^{p}O-<u>*Me*</u>), 56.1 (q, , Ar-^{m}O-<u>*Me*</u>), 55.4 (q , C7-OCH_2O<u>*C*</u>H3), 47.8 (d, C-7'), 27.9 (q, 3C, *t*Bu).

3.8 *tert-Butyl (5R*,8S*)-8-(methoxymethoxy)-5-(3,4,5-trimethoxyphenyl)-5,8-dihydronaphtho[2,3-d][1,3]dioxole-6-carboxylate (**8**)*

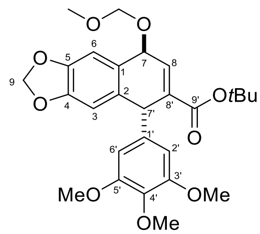

8

Preparation

A tubular Schlenk flask was dried using a heat gun under vacuum. The flask was filled with nitrogen atmosphere. Hoveyda-Grubbs II catalyst (242 mg, 0.386 mmol, 0.2 equiv.) was added, along with a magnetic stirring bar and the flask was put on a vacuum pump for 5 min after which the nitrogen atmosphere was restored. The diene **6** (1020 mg, 1.930 mmol) was dissolved in 4 mL of dry benzene and injected into the flask. The reaction mixture was subjected to 5 cycles of reducing pressure to the boiling point of benzene, allowing for a few seconds of boiling, and then relieving pressure with nitrogen. The reaction apparatus was then placed to an oil heating bath set to 70 °C for 3-4 days, during which NMR analysis was performed daily. When the conversion reached its maximum according to NMR, the reaction was removed from the heating bath. The reaction mixture was then placed on a column (SiO_2, 8 cm in length and 2.5 cm in diameter) and eluted with 15% EtOAc:PE. Green precatalyst was eluted first, followed by 500 mg of clean product (51 %).

R_f = 0.45 (EtOAc:Hex 1:3) **IR** $\tilde{\nu}$[cm^{-1}] (m/z , rel. intensity): (2935-2837 b), (1705, m), (1502, w), (1483, m), (1459, m), (1302, s), (1231, s), (1142, vs), (1123, s), (1035, m), (1007, s), (934.23, m), (848, w), (736, w); **MS (**ESI+) (m/z , rel. intensity): (1023.4, 10, [2M+Na]$^+$), (537.2, 15, [M+2H_2O+H]$^+$), (523.2, 100, [M+Na]$^+$); **HRMS** (ESI+) m/z: calcd for $C_{27}H_{32}O_9Na$: 523.1938 found: 523.1929; **^{1}H NMR** (400 MHz, C_6D_6): δ = 7.56 (dd, J = 2.7, 1.0 Hz, 1H, H-8), 7.25 (d, J = 0.8 Hz, 1H, H-6), 6.76 (s, 1H, H-3), 6.49 (s, 2H, H-2', H6'), 5.43 (ddd, J = 3.4, 2.6, 0.7 Hz, 1H, H-7), 5.30 (d, J = 1.4 Hz, 1H, H-9a), 5.23 (d, J = 1.4 Hz, 1H. H-9b), 5.10 (d, J = 3.6 Hz, 1H, H-7'), 4.71 (d, J = 7.0 Hz, 1H, C7-OC<u>*H*</u>$_a$H$_b$OM), 4.59 (d, J = 7.0 Hz, 1H, C7-OCH$_a$<u>*H*</u>$_b$OCH_3), 3.76 (s, 3H, C7-OCH_2OC<u>*H*</u>3), 3.35 (s, 6H, Ar-^{m}O-Me), 3.22 (s, 3H, Ar-^{p}O-Me), 1.30 (s, 9H, C(C$\underline{H}_3$)$_3$; **^{13}C NMR** (400 MHz, C_6D_6): δ = 165.0 (s, C-9'), 153.9 (d, 2C, C-3', C-5'), 147.9 (s, C-4/5), 147.1 (s, C-4/5), 139.4 (s, C-1'), 138.9 (s, C-4'), 136.2 (s, C-8), 135.2 (s, C-8'), 131.5 (s, C-1/2), 127.3 (s, C-1/2), 108.1 (d, C-3), 106.9 (d, C-6), 106.0 (d, 2C, C-2', C-6'), 100.8 (t, C-9), 96.1 (t, C7-O$\underline{C}$H$_2$OCH$_3$), 74.9 (s, $\underline{C}$(CH$_3$)$_3$), 72.1 (d, C-7), 60.1 (q, Ar-^{p}O-$\underline{Me}$), 55.5 (q, 2C, Ar-^{m}O-$\underline{Me}$), 55.5 (q, C7-OCH$_2$O$\underline{C}$H$_3$), 46.0 (d, C-7'), 27.6 (q, 3C, C($\underline{C}$H$_3$)$_3$).

4 Results and discussion

The first step of the retrosynthesis of **1** is the opening of the D ring in the sense of retro-lactonization which results in a hydroxymethyl group and a carboxylic function both attached to the C ring at the 8 and 8’ positions respectively (see Scheme 9). The next step is the retro-conjugate addition of hydroxymethyl synthon to position 8 which results in a double bond in 1,4 position toward the ester group. Disconnection of 8-8’ results in C-ring opening and disclosure of 2 phenylpropanoid units from which **1** is composed of. RCM leaves two double bonds in close proximity. Bond 2-7’ disconnection reveals two starting parts of the molecule.

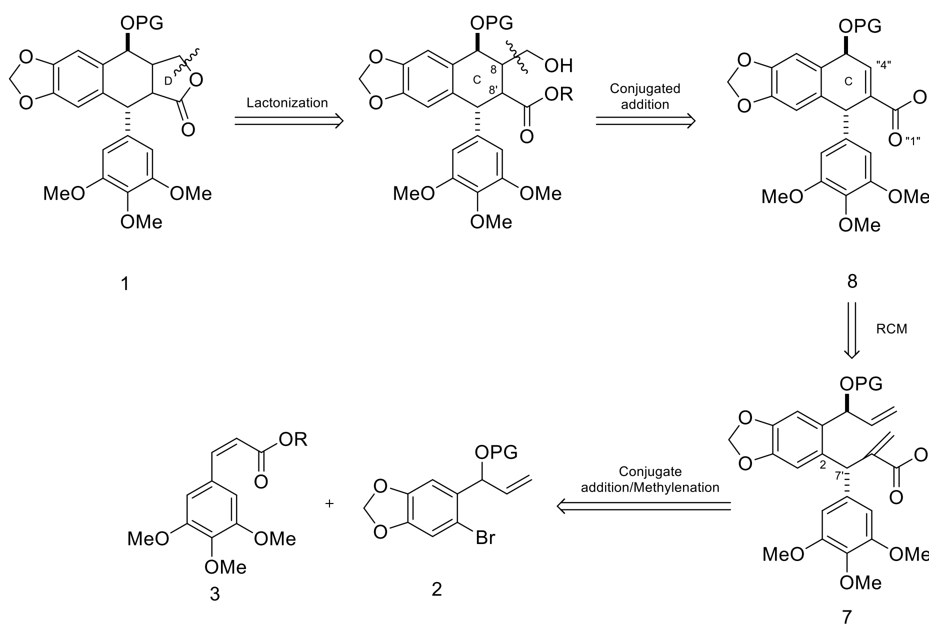

Scheme 9: Retrosynthetic proposal, retro-lactonization, retro-conjugate addition.

Starting material of the whole synthesis is 2-bromo-piperonal which is prepared from piperonal found in natural plants such as vanilla, dill, or black pepper. Piperonal can be prepared by oxidative cleavage of isosafrole. Due to the broad usage of piperonal in MDMA manufacturing, it is a Category I precursor under regulation no. 273/2004 of the European Community, but 2-bromo-piperonal is commercially available.

The first step involves the addition of vinylmagnesium chloride to 2-bromo-piperonal substrate. To facilitate this reaction, DIPEA was added as a non-nucleophilic basic agent, which helps to maintain suitable reaction conditions. Additionally, TBAI was included in the reaction mixture to serve as a catalytic source of iodine, which can accelerate the reaction rate. TBAI is an iodide salt, which can be utilized by Finkelstein reaction to interchange bromine for iodide in our substrate **2**, forming much more reactive specie. The reaction proceeded at 0 °C. The substrate underwent nucleophilic addition to carbonyl leaving secondary alcoholate that was stabilized with DIPEA. After all Grignard reagent reacted, MOMCl was added for the protection of free alcohol generated in this reaction. Protection is important for following steps of this synthesis. This reaction proceeded one-pot in a racemic manner. Yield can be as high as 92% which is satisfactory to the first reaction in synthetic sequence. The racemic molecule was used for the optimization of all following steps.

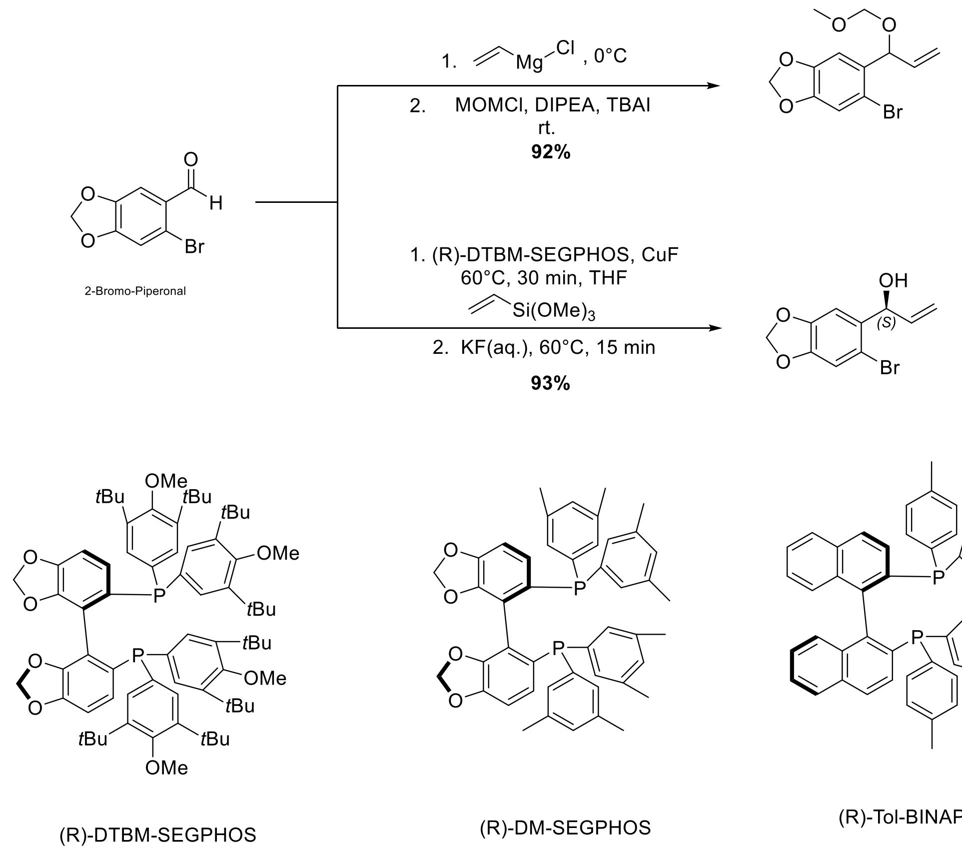

Scheme 10: Enantioselective and regular vinylation of starting material with used ligands for enantioselective vinylation.

Enantioselective alkenylation previously reported on aldehydes leading to chiral allylic alcohols was utilized. Authors demonstrated methodology on various substrates including piperonal[32]. The extra bromine atom at the position close to the reaction center in **2** is causing the molecule to be more sterically hindered but still should be similar enough to undergo reaction under the conditions stated in the article. It was reported that silylated nucleophiles, such a trimethoxyvinylsilane, which are being used in our reaction are activated by a catalytic amount of CuF, forming vinyl coppers through transmetallation. The species can perform enantioselective addition when modified with a chiral phosphine ligand. This catalytic enantioselective method for chiral allylic alcohol synthesis can provide close to quantitative yields with very high enantiomeric excess values.

Our first efforts for reproduction of the method for 2-br-piperonal were accompanied by the usage of Tol-BINAP which yielded 30% and 40% ee (Table 2, Entry 1) even though the reaction utilizing this catalyst should have yielded much higher values. Increasing the number of equivalents of trimethoxyvinylsilane didn't improve reaction yield at any extent. Increasing equivalents only caused the workup to be extremely laborious, as it generated a large amount of silyl polymer residue that had to be removed during the workup. The possible explanation for such low yields could be that product had been locked inside the silyl polymer which was filtered out during the workup. For the disproof of that, harsher hydrolysis methods utilizing TBAF mentioned in the article were tested, although no significant differences were observed (Table 2, Entry 2). After using KF aqueous solution for hydrolysis, we were able to perform a considerably cleaner workup, but yields were still similarly low (Table 2, Entry 4). DTBM-SEGPHOS was described by the authors as the first-rate ligand affording the highest yields and ee values for this reaction, but it also didn't provide any significant improvement during initial experiments (Table 2, Entry 5). A further optimization step was the increase of the loading of CuF, but it neither provided any significant improvement. Our attempts to optimize the reaction led to the strict oxygen-free conditions that were necessary for the reaction to work as reported in the article. The reaction required degassed solvents and strict oxygen-free conditions during the whole process of reaction which afterward yielded 93% with ee values of 94% and 98% after recrystallization (Table 2, Entry 6). This outcome was comparable with the results from the published article. Compound **2e** crystallized as a single enantiomer and was recrystallized for the enrichment of enantiomer using a heptane/EtOAc mixture in a ratio of 1:1. The absolute configuration was determined by X-ray crystalography from the obtained crystal from recrystallization. 7-Hydroxyl was found to be in *S*-configuration.

*Figure 15: 3D structure of **1** obtained by single crystal X-ray method.*

Entry	yield [%]	ee	Ligand	Ligand [%^{mol}]	$C_5H_{12}O_3Si$ [equiv.]	Workup method
1	30	Not measured	(R)-Tol-BINAP	4.0	3	EtOAc/water
2	31	40 %	(R)-Tol-BINAP	6.3	7[(a)]	TBAF method
3	~0	/	(R)-DTBM-SEGPHOS	4.0	6[(a)]	TBAF method
4	6	Not measured	(R)-DTBM-SEGPHOS	5.0	9[(a)]	KF method
5	~0	/	(S)-DM-SEGPHOS	8.0	8[(a)]	Direct silica filtration
6[(b)]	93	98 % (recrystallized)	(R)-DTBM-SEGPHOS	6.3	2	KOH (aq.)
7[(b)]	>90	92 %	(R)-DTBM-SEGPHOS	6.3	2	KOH (aq.)

Table 1: Progress during the optimization of enantioselective vinylation. Column Air states if the reaction has proceeded under oxygen-free conditions. All entries were carried out at 3.7 mol% of KF. (a) Equivalents were added gradually (b) The compound was prepared without access to oxygen.

The Horner-Wadsworth-Emmons reaction was utilized for the preparation of compound **3**. 3,4,5-trimethoxybenzaldehyde was transformed into the cinnamate-like unit with ethyl-2-dimethoxyphosphoryl acetate and *t*BuOK as a base for deprotonation of the acetate at room temperature. This olefination reaction is an approach leading preferentially to *trans* isomer. The reaction is being used for the formation of *t*Bu cinnamate motive needed for the formation of C, D and E-ring. The reaction yielded only 38% which probably caused the hydrolysis of a product forming carboxylic acid during the reaction, which passes to the aqueous phase during workup.

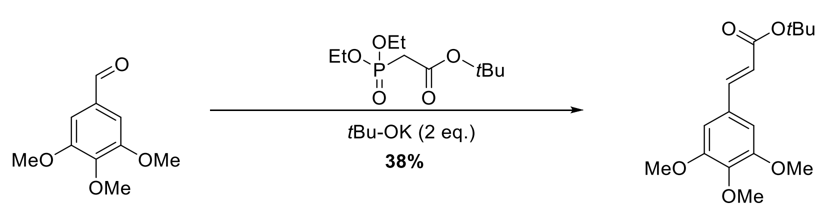

trimethoxybenzaldehyde

3

*Scheme 11: Preparation of **2** utilizing Horner-Wadsworth-Emmons reaction.*

The two major building blocks **2** and **3** were combined in the process of conjugate addition. Bromide **2** was exposed to *n*-Bu-Li undergoing metal-halogen exchange forming a highly efficient organolithium nucleophile. This reactive specie was in the toluene with TMEDA as an intramolecular chelation agent. These conditions let nucleophile to be added to the α,β-unsaturated cinnamate **3** in the 1,4 manner. The reaction had to be optimized for a good diastereomeric ratio. Humidity or presence of ether or other Lewis bases played an important role in the reaction, both compounds had to be dried by dissolving reagents in dry toluene or dry benzene and *in vacuo* evaporation. The solvent formed an azeotrope with volatiles, and was distilled out. The dry conditions led to a more stereoselective reaction. Diastereoselectivity can be explained by the major role of TMEDA and MOM protection group as intramolecular chelator. Levis base probably distorted the chelation system letting the nucleophile attack from any side (see Scheme 12). The clean reaction yielded a diastereomer ratio of 5.5:1 whereas initial efforts without employing clean method achieved dr of close to 4.5:1. The reaction yielded at maximum of 60%.

Toluene is crucial for the reaction to work as it is a non-basic solvent that does not coordinate organolithiums. No product could be obtained while using THF. TMEDA was used for the disaggregation of organolithiums forcing them to act monomer-like and for saturation of 4 lithium's coordination sites (see Scheme 12). The proposed 5-membered metallacycle is formed by two ether oxygens of the MOM group and the carbonyl oxygen from cinnamate **3**. The presence of the MOM protecting group therefore mediated internal nucleophile delivery and caused preference for one certain relative configuration, which was unknown at this point. Relative configuration was elucidated with a compound **8.**

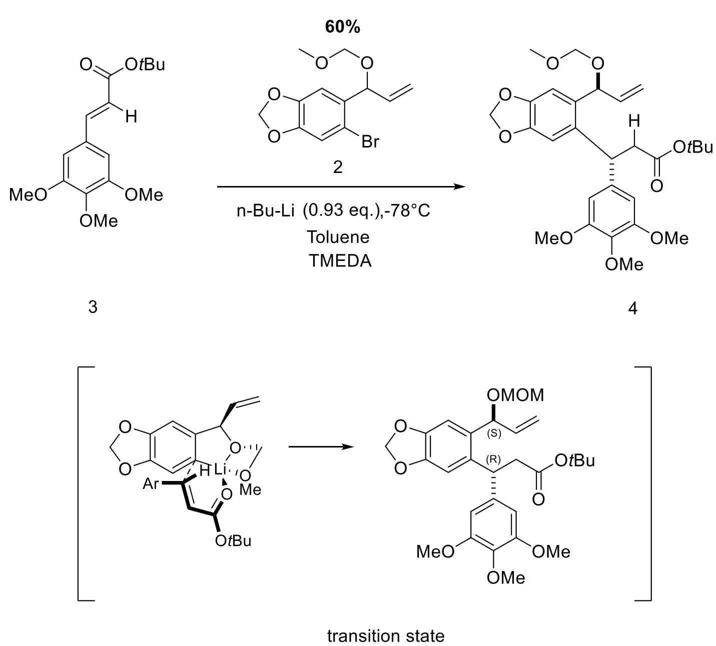

*Scheme 12: **2** and **3** as a building blocks for conjugate addition in toluene and proposed transition state of the formation.*

Methylene moiety needs to be added to ester **4** for the purpose of olefin metathesis. A one-carbon synthon had to be added to position 8’ in ester **4**. Position 8’ can be deprotonated by a strong base such as a LDA or LiTMP forming an enolate that can attack electrophiles. Eschenmoser’s salt is a suitable electrophile that can be eliminated forming a methylene unit.

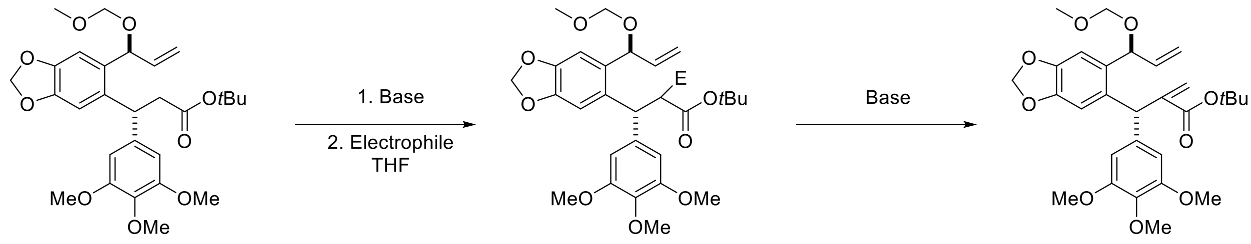

4 5/6 7

*Scheme 13: Deprotonation of **4** and nucleophilic addition to electrophile followed by electrophile adduct elimination toward alkene 7.*

There was an attempt to combine two reactions making the reaction one-pot. The first two reactions gave close-to-zero yield (Table 3, Entry 1,2), which was later explained by the strength of base for elimination. DBU was not strong enough to eliminate Eschenmoser’s salt aduct. Yield increased to approx. 25% after treatment with *t*BuOK (Table 3, Entry 3). Refluxing the reaction mixture in THF for 2 hours afforded some product, but the reaction conditions were too harsh, so the double bond migrated to a thermodynamically more stable position 7’ (Table 3, Entry 4). Excluding refluxing still didn’t provide sufficiently high yield. Reaction was considered unoptimizable.

Entry	Electrophile	Yield	Temperature	Base	Comment
1	Eschenmoser’s salt	<10%	-78 °C for enolization and electrophile add., then rt overnight	DBU	
2	Eschenmoser’s salt	0	-78 °C for enolization, 0 °C, -78 °C electrophile add., then rt overnight	DBU	
3	Eschenmoser’s salt	25%	-78 °C for enolization and electrophile add., then rt overnight	DBU, *t*BuOK	*t*BuOK introduction
4	Eschenmoser’s salt	0	-78 °C for enolization and electrophile add., then refluxed for 2 hours	*t*BuOK	double bond migration
5	Eschenmoser’s salt	10% NMR	-78 °C for enolization, then rt, -78 °C electrophile add., then rt overnight	*t*BuOK	

Table 2: All entries were accompanied by one-pot lithiation, electrophile addition, and elimination. LiTMP was used as a base for deprotonation.

One-pot reaction was divided into 2 parts: the deprotonation with electrophile capture and the elimination of electrophile adduct. MOM chloride was chosen as a potentially good electrophile. Various temperature profiles were tested for the optimization of LiTMP formation, increasing the temperature to 0 °C assured quantitative conversion of TMP and BuLi into LiTMP, which were able to deprotonate **4.** The molecule was probably too sterically inaccessible, and the reaction never yielded more than 42% (Table 4, Entry 2). Various bases such as LDA, KHDMS, and NaHDMS were tested without any improvement.

Entry	Electrophile	Yield	Base	Temperatures	Comment
1	MOMCl	35%	LiTMP	-78 °C to -50 °C for enolization, -78 °C then rt overnight for electrophile add.	
2	MOMCl	42%	LiTMP	-78 °C for enolization, then 0 °C, then -78 ° for electrophile add., then rt 40 min	
3	MOMCl	30%	LiTMP	-78 °C for enolization, then rt, then -78 °C, then 0 °C, then rt (overnight) for electrophile add.	Problem with LiTMP enolization
4	MOMCl	~ 40%(NMR)	NaHMDS	-78 °C for enolization, then rt, -78 °C for electrophile add., 0 °C, then rt overnight	
5	MOMCl	0	KHMDS	-78 °C to 0 °C for enolization, -78 °C for electrophile add., then rt (40 min)	
6	MOMCl	~ 0	LDA	-78 °C to 0 °C for enolization, then -78 °C for electrophile add., then rt	

Table 3: Reaction optimization utilizing MOMCl as an electrophile.

Compound **4** was too sterically inaccessible for any base and therefore deprotonation couldn't proceed to a satisfactory extent. The optimization for higher yields utilizing doable conditions is not possible. The conjugated addition reaction forming **4** proceeds through enolate at the exact 8' position, which can be used as a nucleophile for the attachment of Eschenmoser's salt or any other electrophile. The conjugated addition reaction was therefore not quenched with water, but Eschenmoser's salt was used instead, serving as a quencher of the reaction affording desired product.

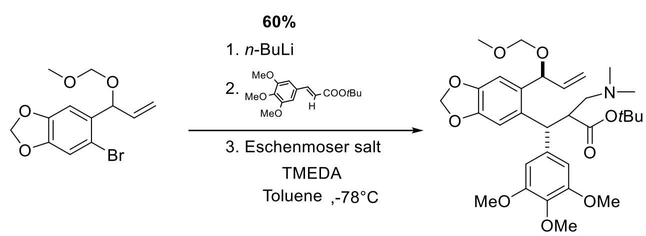

2

5

Scheme 14: Reaction with an electrophile as a quencher.

Reaction worked and improved yields up to 60%, which is same as the reaction quenched with water. This breakthrough shortened the reaction sequence by 1 step and removed problems with challenging deprotonation. Eschenmoser's salt was chosen as a good electrophile. The adduct could be easily transformed into a methylenated molecule by prior transformation to the quaternary salt utilizing methyl iodide and subsequent elimination with *t*BuOK, which yielded 83%.

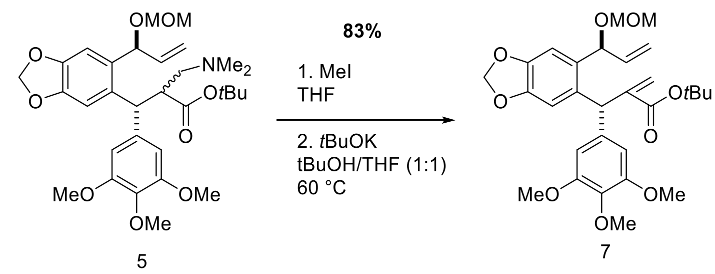

*Scheme 15: Methylation and elimination of **5** toward **7**.*

Ester **7** can be used as a substrate for RCM. The explorational reaction was done on a scale of 10 mg in an NMR tube. The reaction was left for 3 days at 55 °C in a water bath. It took a couple of hours for the catalyst to initiate, which can be recognized by a color change from dark green to non-transparent black.

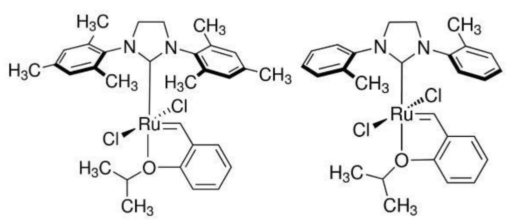

Figure 16: Catalysts used in olefin RCM, left: Hoveyda Grubbs II (M720), right: Hoveyda-Grubbs M721.

The reaction was measured at least daily. Two catalysts were used: HG II and HG M721 with no significant differences observed. It took HG M721 more time to initiate before the process of double bond fusion could take place. Yields were almost quantitative at a small scale reaching up to 99 % which was determined by the preparative TLC. The reaction was later upscaled and yields dropped to range between 40% and 60%. Upscaled reactions reached the highest loading of 1020 mg of compound **7** corresponding to a yield of 51%.

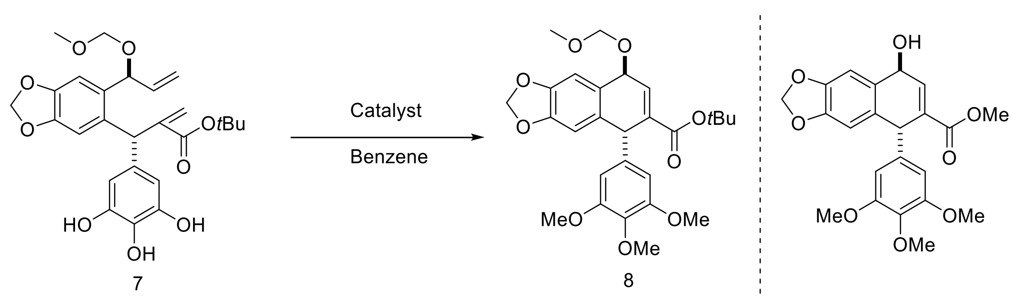

Scheme 16: RCM reaction.

The relative configuration of 7 and 7' was determined by the NMR comparison. Decisive peaks of our substrate **8** share similar chemical shifts and coupling constants with methyl ester derivative synthesized by Linker, which has the following relative configuration of 7 and 7'.

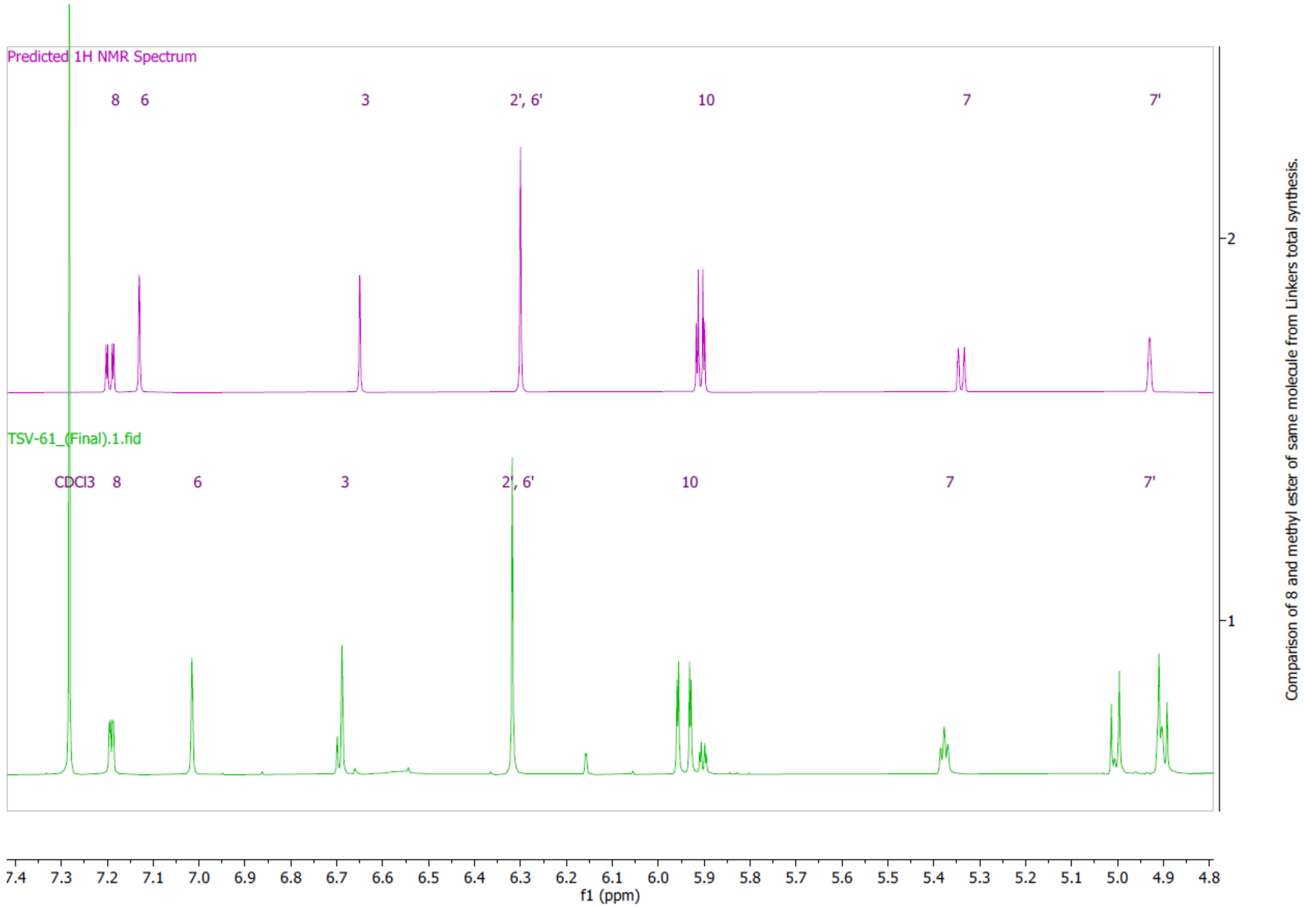

*Figure 17: NMR spectra determining relative configuration of our molecule. Top (violet) spectrum shows chemical shifts meassured by Linker, that belongs to methyl ester derivative of **8**. Bottom (green) spectrum belongs to **8**.*

For the finding if a single addition of whole loading of catalyst at once or partial addition over some period of time matters, product:starting material ratio was analyzed and plotted over reaction time. The first reaction with a single addition of catalysts pursued the biggest conversion progress during the first day (blue line) and then it followed the asymptote limited to a value of ratio close to 1. On day 4 the reaction was quenched for the reason of the non-active catalyst and slow reaction conversion showing that the reaction came to an end.

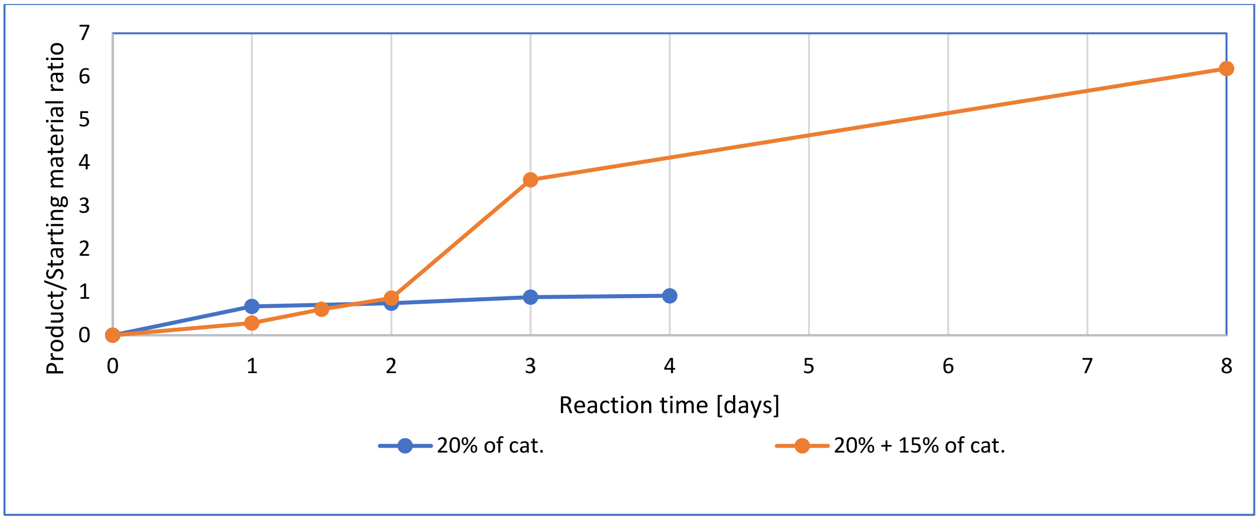

Graph 1: Metathesis reaction, 20%mol catalyst loading, 4-day reaction time, 55 °C, deuterated benzene as solvent.

The same amount of catalyst was loaded to the second reaction and the day 1 and 2 were progressing similarly. Another 15 mol% of catalyst was added on day 2, and the ratio increased to 6-fold higher values. The proposed explanation for this behaviour is the degradation of the catalyst by oxygen dissolved in the initial solvent. Residual oxygen could lead to the catalyst degradation at early stages, even when the solvent was degassed. All values were obtained as integration values of decisive peaks in ^{1}H NMR spectra.

Reaction time [days]	Ratio of reaction 1	Ratio of reaction 2
0	0	0
1	0.67	0.28
1.5	/	0.60
2	0.74	0.86
3	0.88	3.60
4	0.92	/
8	/	6.18

Table 4: Graph 1 raw data. The ratio was obtained as a fraction of integrations of the product peak and starting material peak from NMR measurement.

The product of the metathesis was unstable and decomposed at room temperature. Decomposition was probably caused by the following mechanism that yields aromatic particle, which was detected.

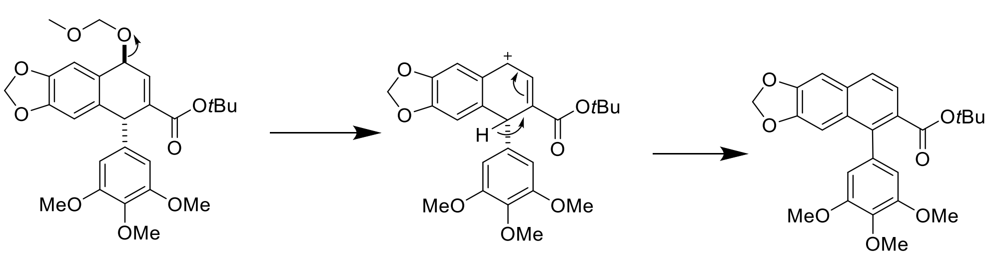

*Scheme 17: Mechanism of **8** decomposition.*

Optimization of conjugate addition to **8** was proposed on an isoelectric and sterically similar model molecule to compound **8**. Compound **3** is a suitable aspirant because it contains an activated double bond next to the ester moiety, bulky tert-butyl ester, and a 3,4,5-trimethoxyphenyl moiety that is also part of **8**. The only difference is the position of the double bond, but it should be easier to proceed with conjugate addition on cyclized molecule **8**.

The next stage of the total synthesis is the addition of the hydroxymethyl group to the double bond via conjugate addition. Because the hydroxymethyl group cannot be added directly, a group that can be easily transformed into hydroxymethyl needs to be added instead. Three nucleophiles were chosen to be added to the double bond. All of which could be then easily transformed into the hydroxymethyl group by Tamao-Flemming oxidation conditions.

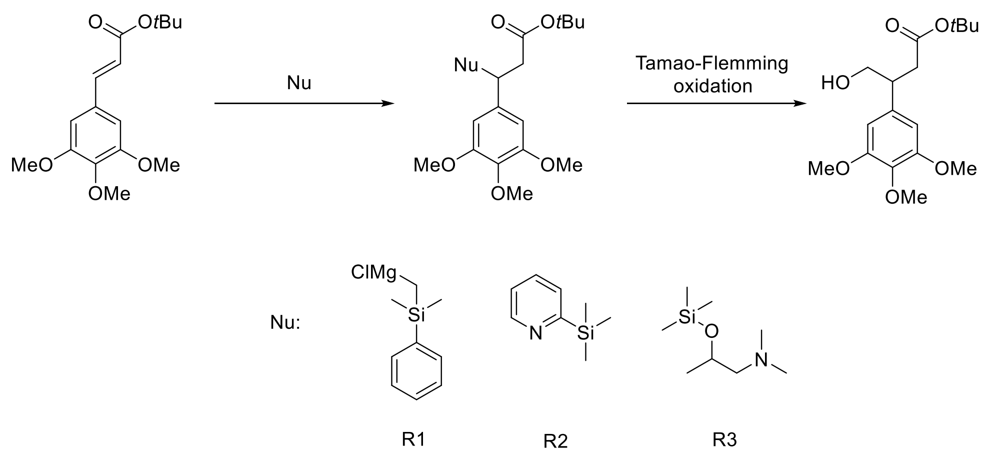

*Scheme 18: Illustration of conjugate addition to **2** and transformation to hydroxymethyl moiety via Tamao-Flemming oxidative conditions. All nucleophiles used in the process are illustrated at the bottom of the scheme.*

Nucleophile R1 was prepared by treating dimethylphenylsilylmethylchloride with magnesium bits in boiling THF. We were not able to add the prepared Grignard reagent to the double bond performing any proposed conditions. Various temperature profiles were tested along with presence of copper (I) in the form of CuBr*Me_2S, but none provided any significant reactivity.

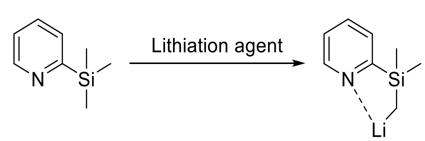

Scheme 19: Lithiation and coordination of Li at 2-TMS-piperidine

Nucleophile R2 was inspired by Itami's paper[33] which stated that the lithiation of 2-trimethylsilyl pyridine deprotonates methyl on the trimethyl silyl group. Anion is then stabilized by nitrogen in close steric proximity. LDA, n-BuLi, t-BuLi, and Ph-Li were tested none of which deprotonated TMS-Pyridine. It was determined by the reaction with benzaldehyde as a good electrophile that no reaction conditions were able to deprotonate our substrate. Not even the exact condition stated in the original paper.

Nucleophile R3 is stabilized by similar coordination. It was prepared by trimethylsilylation of dimethylaminopropan-2-ol and isolated via distillation under decreased pressure.

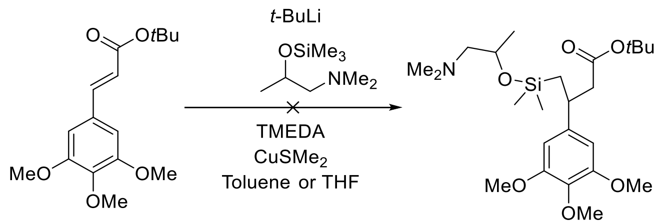

*Scheme 20: Addition of amino alcohol moiety to the model molecule **3**.*

The molecule R3 can be deprotonated well in THF or Toluene with no major problems. Conjugate addition was not fully optimized yet as it did not take place towards the model molecule yet but could be successfully added to the benzaldehyde. Copper and Copper-free approaches were tested with no improvement at all. Low reactivity is probably caused by very bulky tertbutyl moiety on the ester with the combination of high double bond deactivation caused by the present ester group. Reaction conditions still need to be optimized to finish total synthesis.

This potential product can be further oxidized with Tamao-Fleming conditions forming desired hydroxymethyl adduct which can be further lactonized and deprotected forming **1**.

5 Conclusion

The study targeted the development of a new synthetic methodology leading to **1** derivatives. New reactions based on known approaches were modified and optimized for usage with substrates leading to desired products.

Optimization of conjugate addition without electrophile capture was successfully done with better dr achieved. We have never achieved more than approx. 61% yield, by which we can conclude that there is no possibility of better optimization and I conclude that this reaction reached its maximum.

Deprotonation of **4** was explored. Compound **4** is too sterically hindered and so it cannot be successfully deprotonated therefore this reaction is not a good way of obtaining methylenated **4**. Although this reaction led us to the finding that electrophile can be captured one step earlier during conjugate addition and is not necessarily.

Optimization of conjugate addition by using electrophile that can be later eliminated into the methylene moiety shortened reaction scheme by one difficult step and didn't decrease yield to any extent. Elimination was due to knowledge gained from previous unsuccessful experiments during the deprotonation and electrophile addition combined with elimination very straight-forward. The elimination reaction yielded over 80% even with larger loadings of **5/6.**

Olefin metathesis fusing both double bonds present in the molecule was optimized first at a low scale in the NMR tube and later upscaled for large loadings of diene **7.** Reaction at large-scale yielded over 60%. Findings of the importance of loading profiles were explored and we can conclude that it is worth adding catalysts by piece rather than adding the whole amount in one step at the beginning.

All compounds were characterized with modern analytical techniques such as NMR, MS, IR, and TLC. All steps up to conjugate addition of the **8** were successfully optimized and products were characterized resulting in a solid foundation for finishing total synthesis and achieving natural product podophyllotoxin. It was found after tight comparative characterization that the relative configuration of the compound has led to epi-podophyllotoxin, **1** with switched stereocenter at 7. Epi-podophyllotoxin is a starting material for the synthesis of generally used chemotherapeutics Etoposide, therefore our synthesis leads to a widely used therapeutic agent. In conclusion, we were able to fulfill all aims of the work and we will continue in this synthesis until we reach our target molecule.

6 References

(1) Zhao, W.; Cong, Y.; Li, H.-M.; Li, S.; Shen, Y.; Qi, Q.; Zhang, Y.; Li, Y.-Z.; Tang, Y.-J. Challenges and Potential for Improving the Druggability of Podophyllotoxin-Derived Drugs in Cancer Chemotherapy. *Nat Prod Rep* **2021**, *38* (3), 470–488. https://doi.org/10.1039/D0NP00041H.

(2) Shah, Z.; Farooq Gohar, U.; Jamshed, I.; Mushtaq, A.; Mukhtar, H.; Zia-Ui-Haq, M.; Toma, S. I.; Manea, R.; Moga, M.; Popovici, B. Biomolecules Podophyllotoxin: History, Recent Advances and Future Prospects. **2021**, *11*, 603. https://doi.org/10.3390/biom.

(3) Sellars, J.; Steel, P. Advances in the Synthesis of Aryltetralin Lignan Lactones. *European J Org Chem* **2007**, *2007*, 3815–3828. https://doi.org/10.1002/ejoc.200700097.

(4) Linné, C. von. *Species Plantarum : Exhibentes Plantas Rite Cognitas Ad Genera Relatas, Cum Diferentiis Specificis, Nominibus Trivialibus, Synonymis Selectis, Locis Natalibus, Secundum Systema Sexuale Digestas*; Junk: Berlin, 1753; Vol. t.1 (1753).

(5) Borsche, W.; Niemann, J. Über Podophyllin. II. *Justus Liebigs Ann Chem* **2006**, *499*, 59–76. https://doi.org/10.1002/jlac.19324990106.

(6) Schrecker, A.; Hartwell, J. Communications - Components of Podophyllin. XX. The Absolute Configuration of Podophyllotoxin and Related Lignans. *J Org Chem* **1956**, *21* (3), 381–382. https://doi.org/10.1021/jo01109a617.

(7) Lignanların, A.; Ve Bitkiler, Ö.; Dağılımı, A.; Konuklugil, B. *The Importance of Aryltetralin (Podophyllum) Lignans and Their Distribution in The Plant Kingdom*; 1995; Vol. 24.

(8) Kaplan, I. W. Condylomata Acuminate. *New Orleans Med Surg J* **1942**, *94*, 388–390.

(9) Kao, W.-F.; Hung, D.-Z.; Tsai, W.-J.; Lin, K.-P.; Deng, J.-F. Podophyllotoxin Intoxication: Toxic Effect of Bajiaolian in Herbal Therapeutics. *Hum Exp Toxicol* **1992**, *11* (6), 480–487. https://doi.org/10.1177/096032719201100607.

(10) Antúnez-Mojica, M.; Romero-Estrada, A.; Hurtado-Díaz, I.; Miranda-Molina, A.; Alvarez, L. Lignans from Bursera Fagaroides: Chemistry, Pharmacological Effects and Molecular Mechanism. A Current Review. *Life* **2021**, *11* (7). https://doi.org/10.3390/life11070685.

(11) Tóth, G.; Horváti, K.; Kraszni, M.; Ausbüttel, T.; Pályi, B.; Kis, Z.; Mucsi, Z.; Kovács, G. M.; Bősze, S.; Boldizsár, I. Arylnaphthalene Lignans with Anti-SARS-CoV-2 and Antiproliferative Activities from the Underground Organs of <I>Linum Austriacum</I> and

<I>Linum Perenne</I> *J Nat Prod* **2023**, *86* (4), 672–682. https://doi.org/10.1021/acs.jnatprod.2c00580.

(12) Reynolds, R. G.; Nguyen, H. Q. A.; Reddel, J. C. T.; Thomson, R. J. Recent Strategies and Tactics for the Enantioselective Total Syntheses of Cyclolignan Natural Products. *Nat Prod Rep* **2022**, *39* (3), 670–702. https://doi.org/10.1039/D1NP00057H.

(13) Tai, B. H.; Yen, P. H.; Hoang, N. H.; Thanh Huong, P. T.; Dung, N. V.; Van Thanh, B.; Cuong, N. T.; Bang, N. A.; Nhiem, N. X.; Van Kiem, P. New Dibenzocyclooctadiene Lignans from Kadsura Induta with Their Anti-Inflammatory Activity. *RSC Adv* **2022**, *12* (39), 25433–25439. https://doi.org/10.1039/D2RA05052H.

(14) Ohkura, Y.; Mizoguchi, Y.; Morisawa, S.; Takeda, S.; Aburada, M.; Hosoya, E. Effect of Gomisin A (TJN-101) on the Arachidonic Acid Cascade in Macrophages. *Jpn J Pharmacol* **1990**, *52* (2), 331–336. https://doi.org/https://doi.org/10.1016/S0021-5198(19)40068-1.

(15) Antúnez-Mojica, M.; Romero-Estrada, A.; Hurtado-Díaz, I.; Miranda-Molina, A.; Alvarez, L. Lignans from Bursera Fagaroides: Chemistry, Pharmacological Effects and Molecular Mechanism. A Current Review. *Life* **2021**, *11* (7). https://doi.org/10.3390/life11070685.

(16) Lee, J. Y.; Kim, C. J. Arctigenin, a Phenylpropanoid Dibenzylbutyrolactone Lignan, Inhibits Type I–IV Allergic Inflammation and pro-Inflammatory Enzymes. *Arch Pharm Res* **2010**, *33* (6), 947–957. https://doi.org/10.1007/s12272-010-0619-1.

(17) Gnabre, J.; Bates, R.; Huang, R. C. Creosote Bush Lignans for Human Disease Treatment and Prevention: Perspectives on Combination Therapy. *J Tradit Complement Med* **2015**, *5* (3), 119–126. https://doi.org/https://doi.org/10.1016/j.jtcme.2014.11.024.

(18) Zhang, J.; Chen, J.; Liang, Z.; Zhao, C. New Lignans and Their Biological Activities. *Chem Biodivers* **2014**, *11*, 1–54. https://doi.org/10.1002/cbdv.201100433.

(19) Oh, H.-N.; Kwak, A.-W.; Lee, M.-H.; Kim, E.; Yoon, G.; Cho, S.-S.; Liu, K.; Chae, J.-I.; Shim, J.-H. Targeted Inhibition of C-MET by Podophyllotoxin Promotes Caspase-Dependent Apoptosis and Suppresses Cell Growth in Gefitinib-Resistant Non-Small Cell Lung Cancer Cells. *Phytomedicine* **2021**, *80*, 153355. https://doi.org/10.1016/j.phymed.2020.153355.

(20) Gamage, C.; Park, S.-Y.; Yang, Y.; Zhou, R.; Taş, İ.; Bae, W. K.; Kim, kyung keun; Shim, J.-H.; Kim, E.; Yoon, G.; Kim, H. Deoxypodophyllotoxin Exerts Anti-Cancer Effects on Colorectal

Cancer Cells Through Induction of Apoptosis and Suppression of Tumorigenesis. *Int J Mol Sci* **2019**, *20*, 2612. https://doi.org/10.3390/ijms20112612.

(21) Cho, S. J.; Kashiwada, Y.; Bastow, K. F.; Cheng, Y.-C.; Lee, K.-H. Antitumor Agents. 164. Podophenazine, 2‘‘,3‘‘-Dichloropodophenazine, Benzopodophenazine, and Their 4β-p-Nitroaniline Derivatives as Novel DNA Topoisomerase II Inhibitors. *J Med Chem* **1996**, *39* (7), 1396–1402. https://doi.org/10.1021/jm950548u.

(22) Fukamiya, N.; Lee, K.-H. Antitumor Agents, 81. Justicidin-A and Diphyllin, Two Cytotoxic Principles from Justicia Procumbens. *J Nat Prod* **1986**, *49* (2), 348–350. https://doi.org/10.1021/np50044a030.

(23) Beers, S. A.; Imakura, Y.; Dai, H.-J.; Li, D.-H.; Cheng, Y.-C.; Lee, K.-H. Antitumor Agents, 99. Synthetic Ring C Aromatized Podophyllotoxin Analogues as Potential Inhibitors of Human DNA Topoisomerase II. *J Nat Prod* **1988**, *51* (5), 901–905. https://doi.org/10.1021/np50059a014.

(24) H. Saito, H. Yoshikawa, Y. Nishimura, S. Kondo, T. Takeuchi, H. Umezawa Studies on Lignan Lactone Antitumor Agents. II. : Synthesis of N-Alkylamino- and 2, 6-Dideoxy-2-Aminoglycosidic Lignan Variants Related to Podophyllotoxin. *Chem Pharm Bull (Tokyo)* **1986**, *34* (9), 3741–3746. https://doi.org/10.1248/cpb.34.3741.

(25) Liu, Y.-Q.; Jing, T.; Qian, K.; Zhao, X.; Morris-Natschke, S.; Yang, L.; Nan, X.; Tian, X.; Lee, K.-H. Recent Progress on C-4-Modified Podophyllotoxin Analogs as Potent Antitumor Agents. *Med Res Rev* **2015**, *35*. https://doi.org/10.1002/med.21319.

(26) Kamal, A.; Laxman, N.; Ramesh, G. Facile and Efficient One-Pot Synthesis of 4β-Arylaminopodophyllotoxins: Synthesis of DNA Topoisomerase II Inhibitors (NPF and W-68). *Bioorg Med Chem Lett* **2000**, *10* (18), 2059–2062. https://doi.org/https://doi.org/10.1016/S0960-894X(00)00407-8.

(27) Botta, B.; Monache, G.; Misiti, D.; Vitali, A.; Zappia, G. Aryltetralin Lignans: Chemistry, Pharmacology and Biotransformations. *Curr Med Chem* **2001**, *8*, 1363–1381. https://doi.org/10.2174/0929867013372292.

(28) Rathore, R.; Weitberg, A. B. Vinca Alkaloids and Epipodophyllotoxins. In *Encyclopedia of Cancer (Second Edition)*; Bertino, J. R., Ed.; Academic Press: New York, 2002; pp 509–512. https://doi.org/https://doi.org/10.1016/B0-12-227555-1/00257-4.

(29) Reynolds, R. G.; Nguyen, H. Q. A.; Reddel, J. C. T.; Thomson, R. J. Recent Strategies and Tactics for the Enantioselective Total Syntheses of Cyclolignan Natural Products. *Nat Prod Rep* **2022**, *39* (3), 670–702. https://doi.org/10.1039/D1NP00057H.

(30) Fang, X.; Hu, X. Advances in the Synthesis of Lignan Natural Products. *Molecules* **2018**, *23* (12). https://doi.org/10.3390/molecules23123385.

(31) Ziegler, K.; Holzkamp, E.; Breil, H.; Martin, H. Polymerisation von Äthylen Und Anderen Olefinen. *Angewandte Chemie* **1955**, *67* (16), 426. https://doi.org/10.1002/ange.19550671610.

(32) Tomita, D.; Wada, R.; Kanai, M.; Shibasaki, M. Enantioselective Alkenylation and Phenylation Catalyzed by a Chiral CuF Complex. *J Am Chem Soc* **2005**, *127* (12), 4138–4139. https://doi.org/10.1021/ja0507362.

(33) Itami, K.; Kamei, T.; Mitsudo, K.; Nokami, T.; Yoshida, J. Pyridyl Group Assisted Deprotonation of a Methyl Group on Silicon: Complex Induced Proximity Effect and Novel Hydroxymethylation. *J Org Chem* **2001**, *66* (11), 3970–3976. https://doi.org/10.1021/jo015528g.